Endovaginal Urethra and Bladder Imaging

7

Andrzej Paweł Wieczorek
and Magdalena Maria Woźniak

Learning Objectives

1. To review available endovaginal three-dimensional (3D) ultrasound techniques in urethral and bladder imaging
2. To appreciate the efficiency of each of the transducers in the assessment of the morphology of the urethra and bladder
3. To see how the technology used in various transducers influences the quality of image and range of available information
4. To demonstrate techniques of examination with each transducer and to offer practical tips (patient position, preparation, method of acquisition)

Introduction

The female urethra is anatomically and functionally a complex organ conditioning urinary continence. Normal anatomy, proper position, and relation of the urethra to the surrounding pelvic floor structures guarantee normal function of the organ [1–3]. Until recently most published studies focused on perineal pelvic floor ultrasound (pPFUS) assessment of the urethra, its hypermobility, and hyper-rotation recognized as factors in the pathogenesis of urinary incontinence (UI) in females. Transperineal 2D/3D/4D approach is however based on the low frequency transducers (3–8 MHz) and has a number of other limitations making analytic assessment of urethral morphology difficult to achieve.

Introduction to pelvic floor diagnostics rotational transducers with perpendicular ultrasound beam formation to examined organs, using high frequency (12–16 MHz), working in 2D/3D modes and with Doppler options opened the opportunity of very detailed assessment of complex pelvic organs, including the urethra. The technical differences among the transducers, various crystals, and modes of acquisition allow for obtaining a variety of focuses in the detailed examination of the urethra. This chapter describes the characteristics of the endovaginal transducers and optimal conditions in the examinations of the urethra.

Equipment, Technology, and Methodology

Endovaginal examinations of the urethra and bladder may be performed with the use of three various types of transducers, each of them involving different beam formation technology. These transducers include rotational mechanical transducer (type 2050 or its newer version type 2052 or 20R3 transducer as a replacement for 2050/2052

A.P. Wieczorek • M.M. Woźniak (✉)
Department of Pediatric Radiology,
University Children's Hospital, Medical University of Lublin, Al. Racławickie 1, Lublin 20-059, Poland
e-mail: mwozniak@hoga.pl

S. Abbas Shobeiri (ed.), *Practical Pelvic Floor Ultrasonography*, DOI 10.1007/978-3-319-52929-5_7

in new scanners BK3000, BK5000) (BK 2052 Anorectal 3D Transducer, BK Ultrasound, Analogic, Peabody, MA, USA), biplane electronic transducer (BK 8848 Endocavity Biplane Transducer), and rotational electronic transducer (BK 8838 3D ART Transducer). Technical characteristics of each of the transducers are discussed here briefly. For a fuller discussion, see Chap. 2.

Patient Position

Patients are placed in a dorsal lithotomy position on a flat couch or gynecological chair while the endovaginal ultrasound (EVUS) is performed. In some patients, particularly those with pelvic organ prolapse (POP), when the scan obtained in the lying position is insufficient to make the final diagnosis, examination in standing position may be helpful. Scanning on a gynecological chair would be recommended for patients who are assessed with the transducer type 8848 and the use of the automatic mover, because the dimensions of the mover do not allow performing the examination on a flat couch.

Patients Preparation

The patients are recommended to have a comfortable volume of urine in the bladder. No patient preparation is required and no rectal or vaginal contrast is used for the examination.

Methodology

The methodology to obtain the image depends on the type of the transducer used. A silicon cover for all the transducers is required. The amount of gel should be adjusted and equally distributed on the whole surface of the transducer, without air bubbles. The transducer is inserted into the vagina in a neutral position to avoid distortion of anatomy due to excessive pressure on surrounding structures. Proper 2D/3D assessment of the urethra with the use of endovaginal approach with each of the above-mentioned transducers is dependent on the proper acquisition in various sections based on different reference points.

BK 2050/2052/20R3 Anorectal 3D Transducer

This rotational 360° mechanical transducer (see specifications in above-mentioned Chap. 2) has two arrays working in the range of frequencies from 9 to 16-MHz. It provides a good topographical overview of the pelvic floor anatomy on the maximal length of 60 mm, which can be obtained during 60 s of automatic acquisition if the best resolution—minimum spacing (0.2 mm)—is chosen. Larger spacing (possible up to 3 mm) shortens the acquisition time and decreases the quality of the image. The transducer enables individual optimization of the image, depending on the selected anatomical structure in focus, e.g., urethra. The acquisition on the length of 60 mm enables visualization of the urethra in axial section from the bladder base (level I, according to Santoro et al. [4]) to distal orifice (defined as level IV). Ability of downward and upward movement of the crystal inside the transducer is manipulated by pressing the buttons on the transducer, which minimizes moving artifacts coming from the operator. Holding the transducer in stable position during the acquisition ensures good quality in the resulting 3D volume dataset. Even a small asymmetry during insertion of the transducer into the vagina and lack of neutral position result in asymmetry and/or compression of the examined organs. The offline assessment of the 3D file requires a 3D viewer and may be performed either in the scanner or in an external computer. The 3D viewer also enables measurement of the examined structures from the recorded 3D file. The 3D file covers all pelvic floor organs, the anterior, middle, and posterior compartments on all levels. Measurements of all pelvic floor structures may be performed in all sections, including very detailed measurements of the urethra [4, 5].

The reference points to maintain symmetry of the image in the axial section for transducer type 2050/2052/20R3 are the rami of symphysis pubis (SP) and the urethra on the screen at 12 o'clock position. The image obtained at this particular section is named the "gothic arch," as previously reported [5] (Fig. 7.1). Review of the 3D file allows good assessment of the urethra, including the differentiation of its three main parts: intramural, mid-urethra, and distal urethra. Tilting of

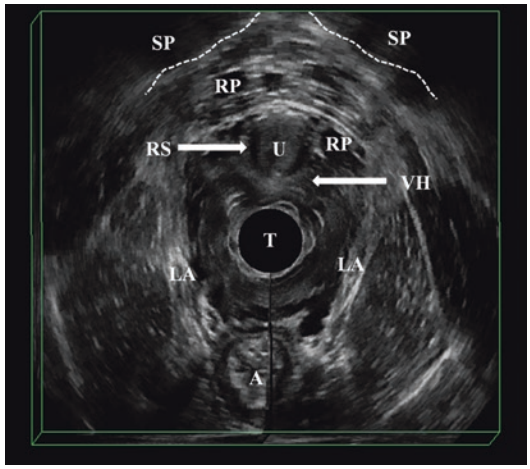

Fig. 7.1 Axial section gray-scale 3D image, transducer BK 8838. Symphysis pubis ("gothic arch")—reference points of symmetry in axial section for transducers 8848, 2050, 2052 and 20R3 (BK Ultrasound). Symphysis pubis (SP), Retzius plexus (RP), urethra (U), rhabdosphincter (RS), transducer (T) in vagina, vaginal hammock (VH), levator ani (LA), anal canal (A)

the acquired 3D image in certain sections may be adjusted to the maximal cross-section and midsagittal axial and coronal section of the particular organ (Fig. 7.2), which allows for obtaining reliable anatomy (see Fig. 7.2b) and reliable measurement. Using the 3D volume dataset recorded during the examination, all required measurements of the urethra and its surrounding structures may be reliably performed.

The main advantage of this transducer is the large region covered during acquisition (360°, all compartments), which provides an excellent overview of all pelvic floor organs, making this transducer universal for many specialties and many purposes. An important feature is the wide selection of scanning time and the quality of obtained image. The universal character of the 2050/2052/20R3 transducer makes it a gold standard diagnostic tool in proctology [6, 7] and for pelvic floor diagnostics, as described in 2009 by Santoro et al. [4, 5, 8].

The main limitation of this technology is the total length of the transducer (54 cm), which is not particularly handy, difficult to operate, hard to keep in a stable position, and also often recognized by patients as extremely long, which creates an extra anxiety for the patient. From the methodological point of view, the mechanical character of the transducer does not allow obtaining the same resolution in all sections; only the axial section (the section of acquisition) has the best quality. All other sections viewed in post-processing of the 3D volume dataset have lower resolution.

BK 8848 Endocavity Biplane Transducer

This is an electronic biplane, high frequency 5–12 MHz, multielement high-resolution transducer, working both in 2D and 3D modes with 6.5 cm linear and convex views transducer. (See specifications in the above-mentioned Chap. 2.) The transducer has the focal range from 3 to 60 mm and contact surface in axial section of 127 mm^2, in sagittal section 357 mm^2. High frequency provides high resolution of examined organs, allowing for very good assessment of urethral morphology. It gives the best broad view of anterior and posterior compartments for functional and anatomical studies. This transducer requires an external mover to obtain reliable 3D volumes. The resulting 3D volume dataset of the anterior compartment of pelvic floor may be analyzed in midsagittal, axial, coronal, and oblique sections.

Sagittal Section

The reference organ to maintain symmetry in the sagittal section is visualization of the urethral lumen on the entire length from the bladder neck to the external orifice (Fig. 7.3). A longitudinal array enables obtaining a 2D and 3D volume dataset in a sagittal section as a free-hand acquisition, during maximum time of 13.4 s with minimal spacing of 0.2 mm. Free-hand acquisition may be connected to artifacts due to uneven movement of the hand in time, which may distort the anatomy and create an artificial nonexisting asymmetrical position of urethra and the pelvic floor structures and their abnormal shape. Free-hand acquisition may, however, be performed on a normal flat couch.

To avoid artifacts connected to free-hand acquisition, the examination may be performed with the use of an automatic external mover (as described in the above-mentioned Chap. 2). In order to safely use the mover, the examination

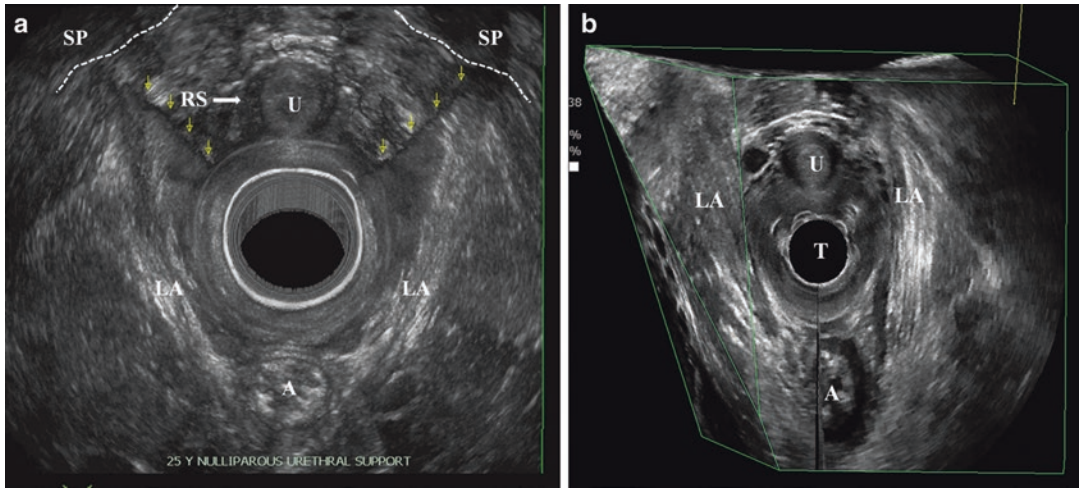

Fig. 7.2 Axial section render mode, transducer 2052 (BK Ultrasound). (**a**) Levator ani and anterior vaginal wall attachments to symphysis pubis (SP). Urethra (U), rhabdosphincter (RS), levator ani (LA), anal canal (A); multisurface 3D reconstruction, transducer type 8838 (BK Ultrasound). (**b**) Attachments of levator ani fibers to symphysis pubis are well demonstrated on oblique sections. Urethra (U), transducer (T) in vagina, levator ani (LA), anal canal (A)

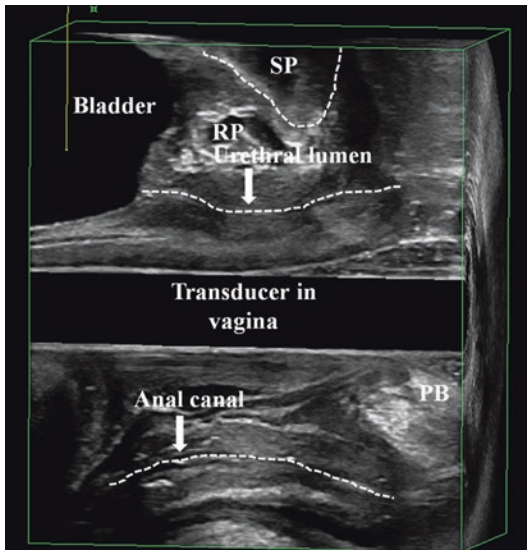

Fig. 7.3 Sagittal section 3D gray-scale image with a biplane 12-MHz transducer (type 8848, BK Ultrasound). Entire urethral lumen from the bladder neck to the external orifice as reference point of symmetry in sagittal section for transducers 8848, 8838, 2050, 2052 and 20R3 (BK Ultrasound). Symphysis pubis (SP), Retzius plexus (RP), perineal body (PB)

must be performed on a gynecological chair. Reproducible 3D studies may be performed with an external mover in both B-mode and in *power*/*color* Doppler modes. With the use of the mover the ultrasound acquisition may be performed in a maximum of 179°, during 46.5 s in B-mode and in 51.2 s in color Doppler mode.

Axial Section

The reference points to maintain symmetry of the image in the axial section is the "gothic arch," the same as in 2050/2052/20R3 transducer (see Fig. 7.1). Any asymmetrical insertion of the transducer to the vagina may cause bias in the obtained image, in the echostructure of the examined organs, and in their dimensions and measurements.

The length of acquisition may be selected by the operator. In the axial section choosing minimal spacing of 0.2 mm the acquisition time of 11.91 s covers 6 cm. The button placed on the transducer switches the image between the two arrays.

The 3D acquisition in axial section may be only free-hand, which may result in inappropriate urethral measurements due to distorted 3D anatomy. This section in 2D and the offline analysis of the 3D volume dataset allow for differentiation of various parts of the urethra such as intramural anatomical elements (layer structure of the trigone, trigonal ring), mid-urethra (differentiation for rhabdosphincter [RS], longitudinal and circular

smooth muscle, submucosal venous plexus), and the distal urethra (fibers of the compressor urethrae), as well as reliable assessment of the urethral relations to external anatomical structures such as the vaginal wall or attachments of levator ani muscle fibers to the SP.

BK 8838 3D ART Transducer

The BK 8838 is an electronic transducer for endovaginal and endoanal/endorectal imaging, with automatic high resolution 3D acquisition transducer. (See specifications in the above-mentioned Chap. 2.) Built-in linear array rotates 360° inside the transducer with no need for additional accessories or external mover. It enables both dynamic 2D and 3D scanning at wide frequency range from 6 to 12 MHz. Its slim diameter (16 mm) is more comfortable for the patient, easy to hold and manipulate for the operator. The 2D scanning plane is controlled remotely from the system keyboard. The image field of 65 mm covers the entire urethra from the bladder base to the external orifice. 2D acquisition can be obtained only in the longitudinal (sagittal) section. The reference section to obtain symmetry is the urethral lumen visualized on the entire length, similar to the reference point for the sagittal section with use of 8848 transducer (see Fig. 7.3). The urethra may be assessed as a separate organ with a small region of interest (ROI), e.g., 45°, or as a part of the entire overview examination of the entire pelvic floor in a 3D file of almost 360° (with a tiny blank stitch), the time of acquisition at maximal length equaling 41.9 s with spacing of 0.4°. The spacing may be changed, which influences the examination time. The electronic character of the transducer allows for assessment of vascularity and flow in *power* and *color* Doppler modes. The Doppler assessment may be performed either as a 2D examination, recorded as a video file on a selected section, or as a static 3D volume dataset.

The axial section may be obtained only in post-processing from the 3D volume dataset. Lack of axial acquisition limits the possibility of using the SP ("gothic arch") as a reference point of symmetry. Inappropriate position of the transducer and B-mode obtained only in the sagittal section may result in asymmetry of the organs in a 3D file (Table 7.1).

Vascular Render Mode and Maximum Intensity Projection

Volume render mode is a technique for the analysis of the information inside 3D–volume by digital enhancing of individual voxels (see Fig. 7.2). It is currently one of the most advanced and computer-intensive rendering algorithms available for computed tomography and can also be applied to high-resolution 3D–US data volume [9]. The typical ray/beam-tracing algorithm sends a ray/beam from each point (pixel) of the viewing screen through the 3D space rendered. The beam passing through the volume data reaches the different elements (voxels) in the dataset. Depending on the various render mode settings, the data from each voxel may be stored as a referral for the next voxel and further used in a filtering calculation, may be discarded, or may modify the existing value of the beam. The final displayed pixel color is computed from the color, transparency, and reflectivity of all the volumes and surfaces encountered by the beam. The weighted summation of these images produces the volume-rendered view [9]. Vascular render mode refers to the application of render mode to 3D data volume with color Doppler acquisition to provide the visualization of the spatial distribution of the vascular networks.

Maximum intensity projection (MIP) is a 3D visualization modality involving a large amount of computation. It can be defined as the aggregate exposure at each point, searching for the brightest or most significant color or intensity along an ultrasound beam. Once the beam is projected through the entire volume, the value displayed on the screen is the maximum intensity value found (the highest value of gray or the highest value associated with a color). The application of MIP in a 3D color mode reduces the intensity of the gray-scale voxels so that they appear as a light fog over color information, which is in this way highlighted. In a color volume the colors are mapped to a given value in the volume.

Urinary Bladder

Specific features of each of the transducer parameters condition the range of obtained anatomical information. However, none of the described

Table 7.1 Endovaginal (EVUS) 2D/3D of the urethra—characteristics of the transducers and reference points

Transducer	Arrays	Sections of acquisition	Type	Frequency (MHz)	Doppler	3D acquisition	Reference points	Range of view	Elastography
2050/2052	Two arrays (low and high frequency crystals)	Axial	Mechanical	9–16	No	Automatic built-in	Gothic arch (axial)	360°	No
20R3 (replacement for 2050/2052 in new scanners BK3000, BK5000)	Each crystal has 3 imaging frequencies	Axial	Mechanical	The multifrequency imaging 9–16	No	Automatic built-in	Gothic arch (axial)	360°	No
8848	Two arrays (linear multielement, transverse multielement)	Axial Sagittal	Electronic	5–12	Yes	Free-hand or external mover	Gothic arch (Axial) Urethral lumen (sagittal)	180°	No
8838	Linear multielement array	Sagittal	Electronic	6–12	Yes	Automatic built-in	Urethral lumen (sagittal)	360° (tiny blank stitch)	No
E14C4t (BK3000, BK5000)	Two arrays simultaneous biplane imaging and endfire imaging in a single transducer	Axial Sagittal	Electronic	4–14	Yes	No	Gothic arch (axial) Urethral lumen (sagittal)	sagittal array 210°; in simultaneous biplane imaging and endfire imaging 140°	Yes

transducers is appropriate for the assessment of the entire urinary bladder due to endovaginal access and the beam formation perpendicular to the organ. The bladder may be visualized only partially, the range depending on bladder filling. The assessment of the entire bladder has to be performed by transabdominal ultrasound or with the use of endovaginal end-fire transducers used widely in gynecology or urology.

In urogynecology, transabdominal assessment of the bladder is needed for the evaluation of the bladder anatomy, its shape (Fig. 7.4), wall thickness, wall continuity, post-void residual volume, in preoperative assessment, and for the exclusion of anatomical abnormalities that might result in urogynecological symptoms. Occasionally, anatomical disturbances such as urachal cyst (Fig. 7.5), bladder diverticula, or ureterocele can mimic tumors of the bladder, particularly if they are localized in the bladder trigone or bladder neck area, and in such cases they can lead to urge incontinence, lower urinary tract infections/symptoms (LUTS), or bladder outlet obstruction. In such cases transabdominal assessment of the urinary bladder should be a part of urogynecological assessment, or any other cases with suspicion of bladder abnormalities. Moreover, if during transabdominal scan of the urinary bladder the asymmetry of the lower part of the bladder in the area of bladder trigone is observed, it may be an indirect sign of lateral levator ani defect due to avulsion.

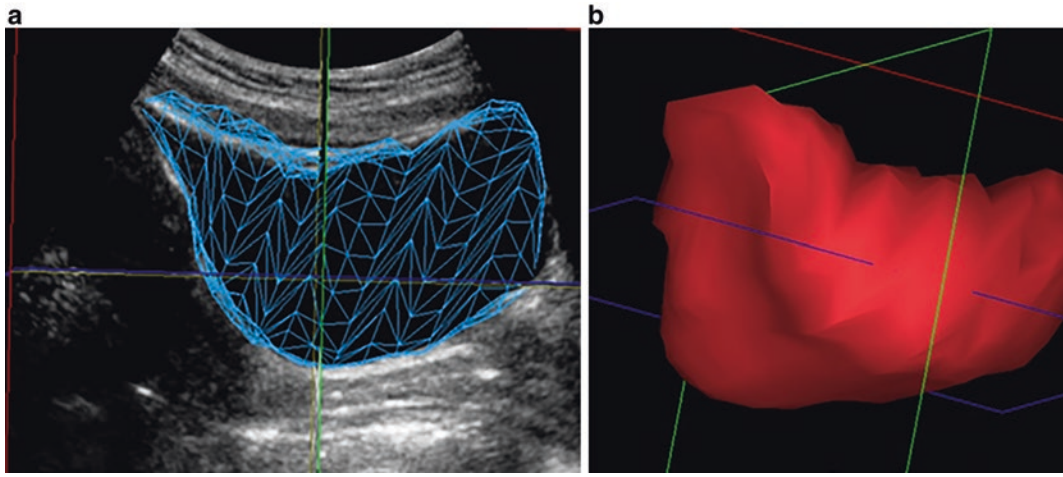

Fig. 7.4 Transabdominal 3D assessment of the urinary bladder; (**a**, **b**) evaluation of bladder shape and post-void residual volume

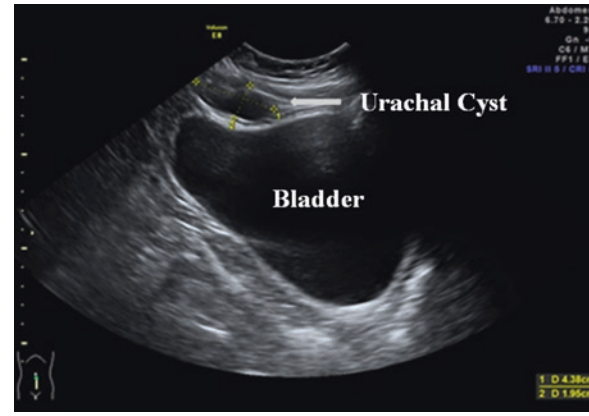

Fig. 7.5 Transabdominal ultrasound of the urinary bladder (B-mode) showing urachal cyst

Anatomy of Female Urethra and Bladder

Ultrasound Morphology

Endovaginal insertion of the transducer can influence the position of examined organs and may limit the reliability of the dynamic studies such as Valsalva and squeeze maneuvers. Stankiewicz et al. proved that in incontinent women with no coexisting POP both ultrasound methods (pPFUS and EVUS) have the same accuracy in the measurements of urethral complex and bladder-symphysis distance (BSD) at rest and during Valsalva maneuver. The study demonstrated that in females suffering from stress urinary incontinence (SUI) and coexisting POP, the endovaginal examination is not reliable in the assessment of the urethral mobility due to alterations of anatomical relations that result from introduction of the transducer into the vagina. Endovaginal approach is more appropriate for detailed assessment of urethral morphology (Fig. 7.6), while pPFUS is the method of choice for dynamic assessment [8].

All described transducers used in EVUS allow proper assessment of ultrasound morphology of the pelvic floor organs, including the urethra and the surrounding structures on different pelvic floor sections and levels as previously defined by Santoro et al. [5, 10]:

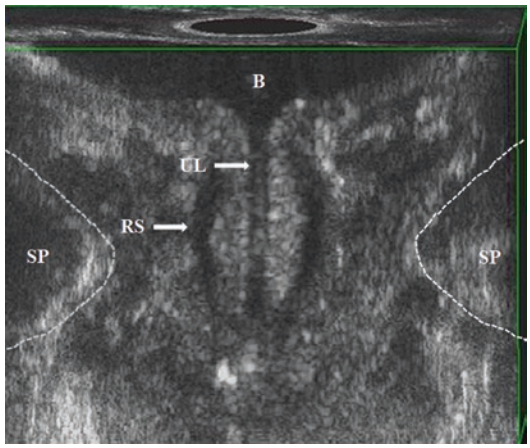

Fig. 7.6 Coronal 3D section showing bladder neck and urethral lumen with a transducer type 2050 (BK Ultrasound). Bladder (B), urethral lumen (UL), rhabdosphincter (RS), symphysis pubis (SP)

Level I: the highest level visualizing the bladder base on the screen at 12 o'clock position and the inferior third of the rectum at 6 o'clock position.

Level II: corresponds to the bladder neck, the intramural region of the urethra, and the anorectal junction.

Level III: corresponds to the mid-urethra and to the upper third of the anal canal. To facilitate the assessment of the position of these structures, a geometric reference point, termed the "gothic arch," was defined at 12 o'clock position, specifically at the point where the inferior branches of the pubic bone join at the SP. At this level, the pubovisceral muscle (PVM) (synonymous with the term pubococcygeus/puborectalis muscle) can be completely visualized as a multilayer highly echoic sling lying posteriorly to the anal canal and attaching to the pubic bone.

Level IV: the outer level, the superficial perineal muscles, the perineal body, the distal urethra, and the middle and inferior third of the anal canal can be evaluated. To visualize these structures in their entirety, the reconstructed axial section should be tilted from the most protruding surface of the SP anteriorly to the ischiopubic rami laterally. In the same scan the urogenital hiatus (UGH) can be evaluated.

The following measurements of the urethra may be performed (Table 7.2 [11]) (Fig. 7.7):
In midsagittal plane

1. Urethral length (Ul) measured from the bladder neck to the external meatus along the urethral longitudinal axis
2. BSD measured from bladder neck to the lowest margin of the SP. According to Wieczorek et al. [11] the mean value of the BSD varied from 33.9 to 34.01 mm, depending on the observer
3. Rhabdosphincter length (RSl) measured in the anterior part of the urethra
4. The distance between bladder neck and RS, corresponding to the intramural part of the urethra

Table 7.2 Measurements of the urethral structures obtained by 3D–EVUS taken by three observers

	Observer 1	Observer 2	Observer 3	
	Mean (SD)	Mean (SD)	Mean (SD)	ICC (95% CI)
BSD (mm)	34.01 (5.1)	33.9 (5.05)	33.9 (5.2)	0.964 (0.931–0.983)
Urethra length (mm)	41.2 (5.6)	40.9 (4.56)	40.7 (5.2)	0.975 (0.918–0.980)
Urethra width (mm)	13.1 (1.44)	13.24 (1.5)	13.1 (1.45)	0.892 (0.801–0.947)
Urethra thickness (mm)	11.6 (1.3)	11.02 (3.2)	11.4 (1.25)	0.848 (0.697–0.929)
Urethra volume (mL)	4.99 (1.3)	5.12 (1.38)	4.82 (1.32)	0.925 (0.86–0.964)
Intramural length (mm)	7.3 (1.7)	7.3 (1.25)	7.5 (1.5)	0.870 (0.764–0.936)
RS length (mm)	18.6 (2.9)	19.1 (2.6)	19.0 (2.6)	0.942 (0.889–0.972)
RS width (mm)	35.3 (4.07)	35.2 (4.1)	34.3 (3.9)	0.85 (0.728–0.926)
RS thickness (mm)	2.4 (0.21)	2.47 (0.23)	2.4 (0.24)	0.611 (0.390–0.789)
RS volume (mL)	1.27 (0.35)	1.28 (0.38)	1.24 (0.32)	0.909 (0.829–0.957)

Statistical analysis: intraclass coefficient correlation (ICC). From Wieczorek et al. [11], with permission

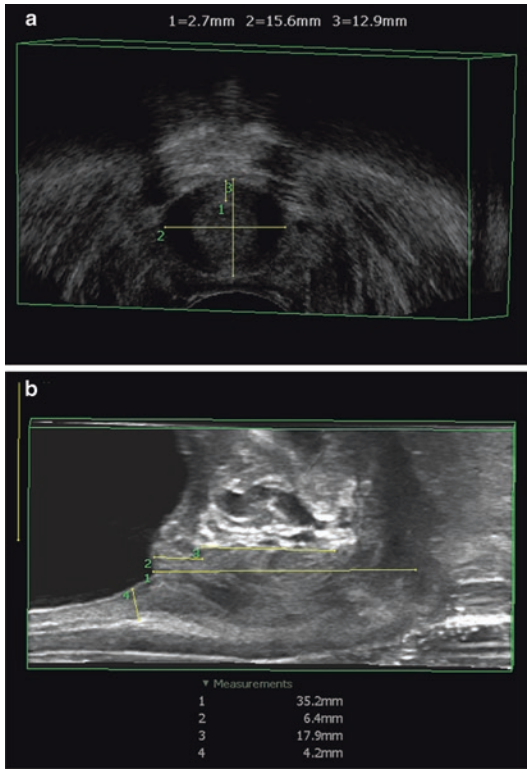

Fig. 7.7 Axial (**a**) and sagittal (**b**) section, 3D gray-scale mode with a transducer type 8848 (BK Ultrasound) demonstrating measurements of the urethra performed in the 3D viewer

In axial plane of the mid-urethra

5. Urethral complex width (Uw)
6. Urethral complex thickness including RS (Ut)
7. Width of the RS measured along its external border, where it is attached with the smooth muscle to the RS raphe—a tissue connection to the anterior vaginal wall (RSw); this is a summing value of the linear measurements performed by the use of tools available in the BK 3D Viewer. The RS appears in the axial section as a slightly hyperechoic (compared with urethral smooth muscle) structure surrounding ventral and lateral sides of the mid-urethra and forming a raphe connected to the anterior vaginal wall. Thus, the RS has its typical omega shape [11]

According to integral theories described by Petros and Ulmsten, between the mid-urethra and the vaginal anterior wall are located the puboure-thral ligaments and the suburethral vaginal hammock [1, 2]. This hammock is attached to the endopelvic fascia, and laterally the urethra is limited by periurethral space, including the Retzius vascular plexus, and by the elements of levator ani. In the section when the levator hiatus is well visible, the paravaginal spaces can also be determined, located between the lateral border of the vaginal wall and the medial border of the PVM. Shobeiri et al. demonstrated levator ani subdivisions visible on 3D EVUS at three levels, where level 2 contained the attachment of the pubovaginalis, puboperinealis, puboanalis, puborectalis, and iliococcygeus to the pubic bone [12]. It is possible to explain deterioration of continence with time in terms of age-related

connective tissue laxity of the vaginal hammock. In time, improvement in continence after anti-continence surgery can be explained by tightening of the hammock via paraurethral scar contraction [13].

Review of the literature shows significant differences in the assessment of the anatomy of the urethra, its dimensions and volume [4, 5, 11, 14–17]. Santoro et al. in the study performed with the high-resolution 3D EVUS 2050 transducer demonstrated urethral length of 38.2 mm; urethral volume of 3.06 mL; and RS volume of 0.45 mL [5]. The results published by Wieczorek et al. [11], performed with the same type of transducer (2050), reported urethral length of 41.0 mm; urethral volume 4.9 mL; and RS volume 1.2 mL. The difference in RS volume between the Santoro and Wieczorek studies results most probably from different mathematical algorithms used for calculating the volume and also the unclear borders in the sagittal section that may be interpreted differently by various operators. Similar results were also found by Shobeiri et al. in the study on anterior and posterior compartment 3D EVUS with the 8848 probe based on direct histologic comparison; urethral length was reported as 36.0 mm [18]. Additionally, Shobeiri et al. obtained the following mean measurements of other pelvic floor structures: striated urogenital sphincter area 0.6 cm^2; longitudinal and circular smooth muscle area 1.1 cm^2; urethral complex width 14 mm; and urethral complex area 1.3 cm^2 (Fig. 7.8). The agreement for visualization of structures was as follows: vesical trigone 96%; trigonal ring 94%; trigonal plate 84%; longitudinal and circular smooth muscle 100%; compressor urethrae 97%; and striated urogenital sphincter 97% [18].

The above results are concordant also with those obtained by Kondo et al., where morphology obtained in transvaginal ultrasonography was confirmed on cadaver specimens. The RS (peripheral zone) thickness was reported in various patients' groups: continent patients, patients with SUI, and patients with urge urinary incontinence, as 2.78, 2.14, and 2.87 mm, respectively [19]. Above results are also concordant with those obtained by Macura et al. in the MR study

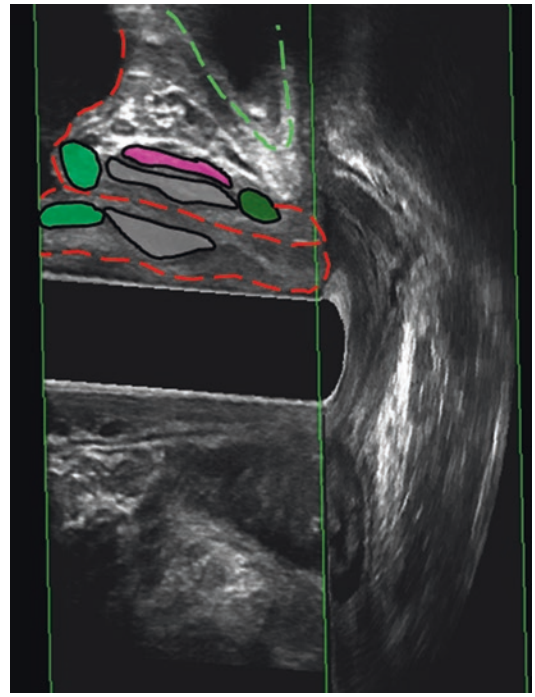

Fig. 7.8 Anterior compartment 3D endovaginal ultrasound anatomy as seen with 8848 probe based on direct histologic comparison

on urethral morphology [20]. These results are slightly different to those obtained by Umek et al., who presented sagittal urethral diameter of 8.4 mm if measured in endovaginal access and 11.5 mm measured from endoanal access, urethral volume of 1.6 mL (both anatomical accesses) and RS volume of 0.7 and 0.8 mL, accordingly [16]. In the study performed by Santoro et al. with the 2050 transducer [4] involving the interobserver, intra, and interdisciplinary reproducibility of pelvic floor measurements, the sole urethral dimension measured was urethral thickness. The results were concordant with urethral dimensions obtained in all the above studies [4]. Moreover, as the study focused mainly on the reproducibility of the performed measurements in EVUS among various specialties (urogynecologists, colorectal surgeons, radiologists) and the operators' different experiences in ultrasound diagnostics, the conclusions from the study were that 3D–EVUS yields reproducible measurements of levator hiatus dimensions and urethral

thickness in asymptomatic nulliparous women. Agreement was best where landmark edges were well defined (levator hiatus dimensions) and acceptable where more reader judgment was needed (urethral thickness in the oblique axial plane). Using standardized criteria, the evaluation of these pelvic floor structures appeared to be independent from the different background training of the readers. The method appeared a reproducible technique for urethral measurements [4].

The RS may be also evaluated during intraurethral ultrasound as reported by Frausher et al. This technique provides excellent high-resolution images and allows for real-time visualization of the sphincter mechanism [21]. The RS thickness for patients with urge incontinence and for patients with combined stress and urge incontinence was reported as 3.2 mm.

However, the volumes of RS given generally in the literature seem to be significantly lower than that reported by Digesu et al. [14] and Derpapas et al. [17]. The study by Digesu et al. demonstrated the RS volume of 3.79 mL in patients with successful surgical procedure due to SUI, while in patients with failures 1.09 mL. In the paper by Derpapas et al. the RS volume was 8.88 mL in black females and 5.97 mL in white females. Both studies were performed from pPFUS access: the study by Digesu et al. was performed with the use of sector, endovaginal transducer, and the study by Derpapas et al. with the 3D/4D curved array probe [14, 17].

The differences may result from the various nomenclature of urethral anatomy treated differently by different authors. There are many controversies in female urethral anatomy that have a significant impact for understanding urinary continence [22]. Variability of obtained results among authors may also result from various frequencies of the transducers used, different anatomical accesses, and various patient groups (age, race, BMI, parity, etc.). The differences in urethral morphology and physiology between black and white women have already been reported in the literature [17, 23]. Howard et al. reported that black women demonstrated differences in ultrasonically measured vesical neck mobility during a maximum Valsalva effort compared to white females (blacks = −17 mm vs. whites = −12 mm). Functional and morphologic differences exist in the urethral sphincteric and support system of nulliparous black and white women [23].

Moreover, the diagnostics of such a small organ as the urethra may relatively easily result in variability of the measurements obtained in various techniques among the authors. Moreover, review of the literature concerning 3D diagnostics of the urethral complex shows that most researchers perform only one acquisition in axial plane to obtain the 3D dataset, which may also potentially influence obtaining reliable measurements in all three planes.

Urethral Vascularity

Vascularity is one of the major factors contributing to maintaining the normal function of the urethra. The vascularity, particularly the presence of cushioning blood vessels within the submucosa, conditions the normal tension of the urethral mucosal wall [24, 25]. Sphincteric closure of the urethra is normally provided by urethral striated muscle, the urethral smooth muscle, and the vascular elements within the submucosa. Each is believed to contribute equally to resting urethral closure pressure [24]. The submucosal vascular systems become engorged with blood, which causes swelling of the submucosa and decrease in the diameter of the urethral lumen [22]. Furthermore, the vascularity system is also responsible for the proper synthesis of factors that influence surface sealing of the urethral lumen.

Up to now, the assessment of urethral vascularity has mainly been based on selected Doppler parameters (velocity [*V*], resistive index [RI], pulsatility index [PI]), measured with pPFUS [26, 27]. Siracusano et al. [27] demonstrated the usefulness of color Doppler and spectral Doppler scans in the assessment of urethral vascularization in healthy young women, defining the RI in urethral vessels at three parts of the urethra (proximal, middle, and distal), and reporting an increased RI in the intramural part of the urethra. Also the attempts of the assessment of vascularity after intravenous contrast agent administration

were undertaken [27, 28] from the transperineal approach. Siracusano et al. performed the examinations after intravenous application of ultrasound contrast in order to enhance Doppler signals from the urethral vessels, which seemed to generate good results. The application of invasive and relatively expensive diagnostic methods such as intravenous contrast agent administration seems to be unnecessary, considering the recent advances in ultrasound diagnostics, particularly in high frequency endoluminal ultrasonography (12 MHz) in urological practice, which can generate an ultrasound beam that is perpendicular to the urethra and in almost direct contact with the organ, thus enabling vascular assessment [29, 30].

The usefulness of color Doppler in the quantitative assessment of urethral vascularity has been already described [29]. The studies performed by Wieczorek et al. [29] demonstrated that high frequency transvaginal ultrasound with the use of color Doppler mode is a very reliable method enabling visualization of urethral vessels distribution. The vascularity differs in different parts of the urethra, with the mid-urethra being the most vascularized part of the organ. Lone et al. demonstrated a significant reduction in the vascularity parameters in all measured variables of urethral vascularity in continent multiparous women compared to continent nulliparous women when parity was accounted for [31]. In another study also published by Lone et al. of women undergoing treatment for SUI, there is no change in blood flow intensity; at 12 months there was no change in vascularity parameters in women who opt for conservative or surgical treatment of SUI [32].

Quantitative assessment of the urethral vascularity can be performed with the use of an independent external software package (Chameleon, Münster, Germany), which has been proved to be a valuable tool for providing reproducible quantitative analysis of vascular parameters for the entire urethra [29, 30]. The analysis is based on video files recorded in color Doppler mode. The video files may be recorded using transducers type 8848 or 8838. The vascular pattern may be obtained both in the sagittal section at the level of urethral lumen and the axial section at the level of mid-urethra with the use of the transducer type 8848 or in the sagittal section at the level of urethral lumen with the use of the transducer type 8838. The data must be registered as video files in a stable position of the probe.

The vascular pattern may be analyzed within manually defined ROIs. The software automatically calibrates distances and color hues as flow velocities and calculates the color pixel area and flow velocity—encoded by each pixel—inside an ROI of a video sequence (20–90 images). Videos with movement artifacts are automatically or manually excluded from perfusion quantification.

In the sagittal section regions of interest could be set at sequence at 3 levels (intramural, mid-urethra, and distal urethra) (Fig. 7.9). In the axial plane two regions of interest could be defined for each patient—one comprising the RS (the outer ring of urethra) and the second comprising the circular smooth muscle, the longitudinal smooth muscle, and the submucosa (the inner ring of the urethra) (Fig. 7.10).

The following parameters may be automatically computed for each single frame of the video within each ROI:

- The velocity (V), corresponding to the color hue of the pixels inside the ROI
- The perfused area (A), given by the number of perfused pixels inside the ROI
- The perfusion intensity (I), defined as the ratio $I = VA/A\mathrm{ROI}$, where AROI denotes the total area of the ROI

In this way, the perfusion intensity increases with the perfusion velocity, but decreases if less of the total area of the ROI is perfused. This parameter is calculated for every image in each video, in order to compute averages and pulsation indices of the parameters, always with respect to the duration of a full cardiac cycle. Inside the ROI, the whole area occupied by the colored pixels is calculated. This calculation is automatically repeated for the same ROI for all images of a digital video. The detection of one full heart cycle is also done automatically by the software.

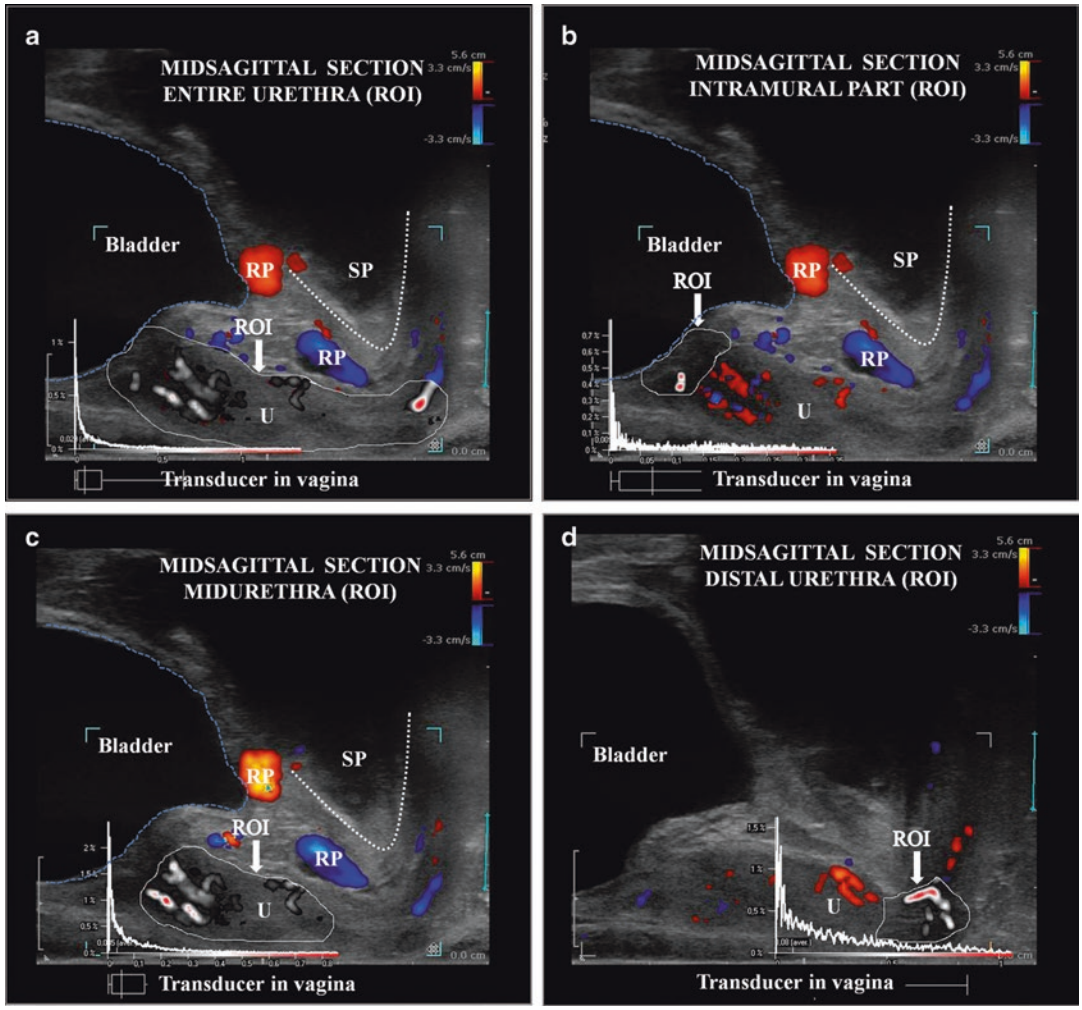

Fig. 7.9 Endovaginal ultrasound with a biplane 12-MHz transducer (type 8848, BK Ultrasound) using linear array. Analysis of the vascular parameters with the use of Pixel Flux software in the longitudinal (sagittal) section. Four regions of interest (ROIs) are defined: at the entire urethra from the bladder neck to the external orifice (**a**), the intramural part of the urethra (**b**), the mid-urethra (**c**), and the distal urethra (**d**). Symphysis pubis (SP), Retzius plexus (RP)

The output is the measure of flow quantity inside the ROI, called "perfusion intensity," calculated in terms of the hue of the pixels in the ROI:

- The pulsatility index (*PI*)
- The resistance index (*RI*)

Each parameter is calculated, including data from all imaged vessels in color Doppler mode coded as red and blue, reflecting the direction and velocity of blood particles movement. Results represent the sum of "red" and "blue" values named as "mix" value for each parameter (Vmix, Imix, Amix, PImix, and RImix.) [29, 30].

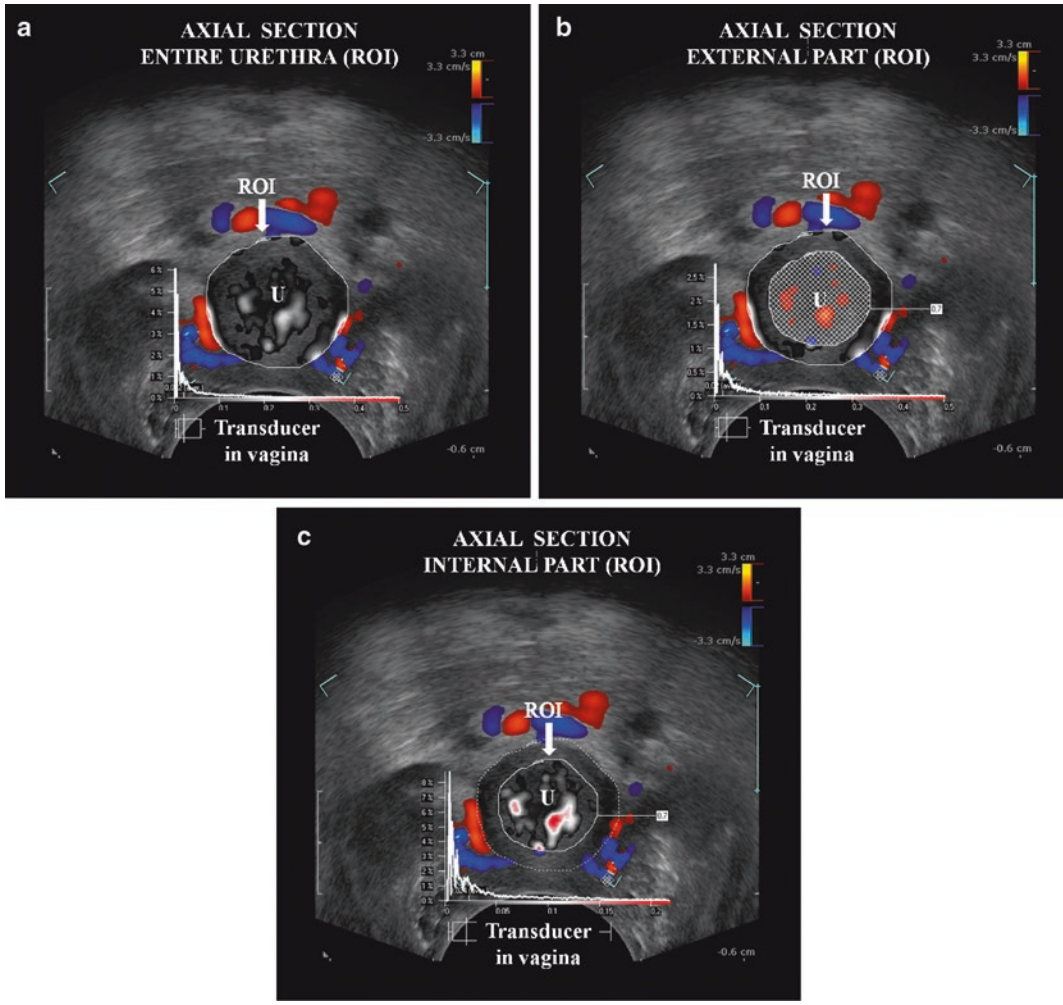

Fig. 7.10 Endovaginal ultrasound with a biplane 12-MHz transducer (type 8848, BK Ultrasound) using transverse array. Analysis of the vascular parameters with the use of the PixelFlux software (Chameleon, Münster, Germany) in the axial section at the level of mid-urethra. Three regions of interest (ROIs) are defined: entire urethra (**a**), the external part of the urethra (rhabdosphincter) (**b**), and at the internal part of the urethra (including the lisosphincter muscle that comprises the circular smooth muscle, the longitudinal smooth muscle, and the submucosa) (**c**)

Clinical Applications of Urethral Ultrasound

According to Chaudhari et al. the introduction of high-resolution surface and intracavitary transducers in conjunction with 3D acquisition has enhanced the role of ultrasound in the diagnostics of the urethra [33]. From the clinical point of view recent advances in ultrasound allow more detailed evaluation of urethral and periurethral abnormalities, enabling categorization of the patients suffering from pelvic floor disorders for various groups, with or without existing anatomical abnormalities. It is very important to define prior treatment and whether or not the cause of the abnormality has an anatomical background or is purely a functional disturbance, as it significantly influences the choice of treatment. Chaudhari et al. stated that in the presence of anatomical pathologies the distinctive imaging features and locations of the various diseases aid in narrowing the differential

diagnosis. Real-time ultrasound has exciting potential as the tool for more comprehensive analysis of the pathophysiologic features of the complex disorders that affect the female urethra and periurethral tissues [33].

There are numerous risk factors for the development of pelvic floor dysfunction, including age, multiparity, history of vaginal delivery, menopausal status, obesity, and history of hysterectomy. Patients present with signs and symptoms that often overlap with those of urethral diverticula and periurethral cystic lesions, including pelvic pain, incontinence, dyspareunia, incomplete emptying, and, at times, visible organ protrusion (Fig. 7.11) [33].

High frequency endovaginal 3D morphology of the urethra can significantly enrich our knowledge about abnormalities that are not clinically evident but may play a role as causative factors of urinary incontinence. According to Wang et al. the urological anatomies can be generally categorized into three types: abnormal communication of urogenital tracts, malformation of bladder or ectopic ureter, and anomalies of urethral orifice. Ectopic ureters and ureteroceles are typically diagnosed in childhood and rarely present in adults. Nevertheless, ureteral ectopia should be included in the differential diagnosis of older patients who present with urinary tract infections or urinary incontinence (Fig. 7.12) [34, 35]. Surgical corrections are helpful for most cases [35]. This has been confirmed by Tunn et al. [36] in updated recommendations on ultrasonography in urogynecology, where he concluded that ultrasonography is a supplementary, indispensable diagnostic procedure and that pPFUS and ERUS are the most useful techniques. In patients undergoing diagnostic work-up for urge incontinence, ultrasound occasionally demonstrates urethral diverticula, leiomyomas, and cysts in the vaginal wall [36]. High frequency high-resolution EVUS allows comprehensive evaluation of both congenital and acquired pathologies, including diverticula, abnormal ureteral insertion, dystopic/ectopic ureters, calcifications, ureterocele, fistulas, and other urethral and paraurethral lesions [37]. Among periurethral cystic lesions, abnormalities such as Gartner duct cyst, Bartholin gland cyst, Skene duct cyst, Müllerian cyst, epidermal inclusion cyst, perineal-vulvovaginal endometriomas, and injected collagen may be diagnosed. It is important for radiologists to be aware of the imaging characteristics of these entities, in particular their location, to differentiate them from urethral diverticula [33]. Although the exact mechanism of diverticular formation is unknown, the most commonly accepted theory implicates the periurethral glands. Obstruction of the periurethral gland duct is associated with infection that results in abscess formation that subsequently ruptures into the urethral lumen forming the diverticulum. Yang et al. showed on two cases of paraurethral abnormalities such as urethral diverticulum and paraurethral abscess that transvaginal sonography, with its high-resolution visualization of the lower urinary tract, may aid in the diagnosis and treatment of such disorders. Using 3D technology, the internal architecture of the paraurethral abnormalities and their spatial relationship to the urethra and bladder, important considerations at surgery are clearly demonstrated on ultrasonography. Complete excision of complex paraurethral anomalies may be per-

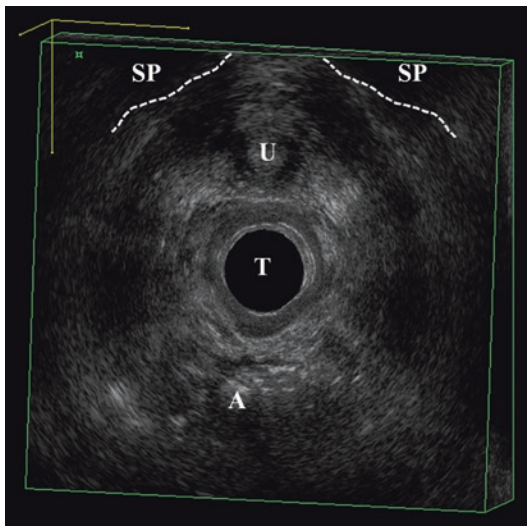

Fig. 7.11 Axial section 3D B-mode with a transducer type 2052 (BK Ultrasound). Urethra (U) and symphysis pubis (SP) in pelvic organ prolapse (POP 3) and urinary incontinence (UI). Lack of differentiation of anatomical pelvic floor structures. Enlargement of urogenital hiatus. Transducer (T) in vagina, anal canal (A)

Fig. 7.12 Gray-scale axial section, transducer 8848 (BK Ultrasound). Dystopic ureter entering the urethra

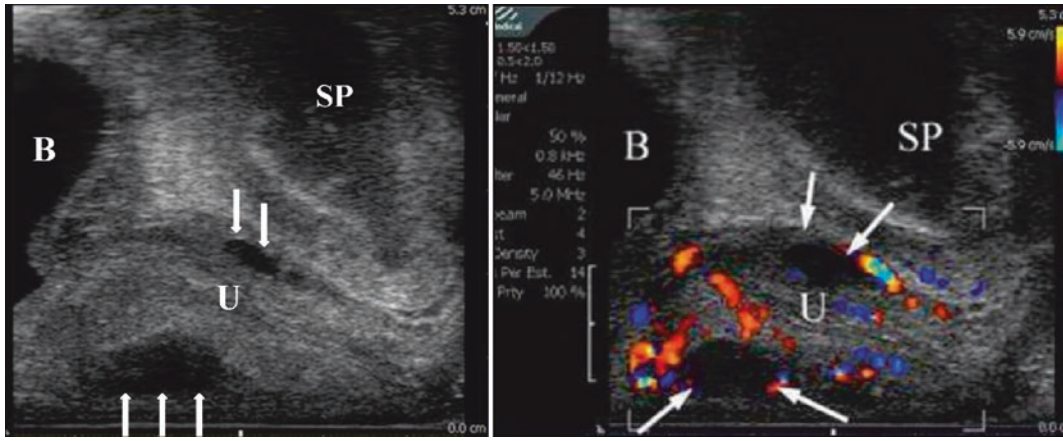

Fig. 7.13 Sagittal section gray-scale (**a**) and color Doppler (**b**) mode with 8848 transducer (BK Ultrasound) demonstrating vaginal diverticula (*arrows*). The image performed in *color* Doppler mode (**b**) presents hypervascularity due to the infection of the diverticula. Bladder (B), urethra (U), symphysis pubis (SP)

formed under transvaginal sonographic monitoring without inadvertent injury to the bladder or urethra [37]. Urethral diverticulum has been reported in 1.4% of women with SUI (Fig. 7.13) [38]. In the total population of females the prevalence of this pathology is estimated to be approximately 0.6–6% [33]. EVUS enables reliable diagnostics of urethral diverticula, preoperative assessment, and, if necessary, the diagnostics of postoperative complications. For preoperative planning, it is vital to evaluate the diverticula in terms of location, size, number, configuration, possible sac contents, mass effect, and position of the neck, resection of which is critical in preventing recurrence [33]. Complications of urethral diverticula include infection, calculus formation, and neoplasm development [33]. EVUS seems to play an important role in the diagnostics of periurethral abscesses. A case report by Huang et al. showed the usefulness of EVUS in the diagnostics of vaginal abscess mimicking a cystocele and causing voiding dysfunction after Burch colposuspension [39]. According to Chaudhari urethral fistulas are divided into urethrovaginal, rectourethral, and urethroperineal subtypes [33]. The study by Rostaminia et al. showed that visualization of periurethral structures by 3D EVUS in midsagittal plane is not associated with SUI status. There were no differences in visualization of defects in the trigonal ring, vesical trigone, trigonal plate, longitudinal muscle, and striated muscle between groups. The authors found no

meaningful statistical difference in the visualization of striated muscle by continence status, but the proportion of striated muscle defect visualized in incontinent women was 21% more than in continent women [40].

EVUS is a very important modality in the algorithm of the diagnostics and monitoring of treatment of urethral tumors (Fig. 7.14) [41]. Urethral leiomyomas are extremely rare, benign smooth muscle tumors that may grow during pregnancy and result in dysuria. A well-defined homogeneous tumor with increased vascularity is the typical ultrasound manifestation. Urethral carcinoma is a rare neoplasm that accounts for less than 0.02% of all malignancies in women. Squamous cell carcinoma (70% of cases) classically involves the distal urethra and the external urethral meatus. Transitional cell carcinoma (20%) and adenocarcinoma (10%) typically involve the proximal urethra. Urethral malignancies exclusively involving the distal third of the urethra are known as anterior urethral tumors, with the remainder of malignancies being referred to as entire urethral tumors [33].

Secondary urethral carcinomas are rare tumors that extend contiguously from the urinary bladder, cervix, vagina, uterus, and anus; the seeding may occur during urethral instrumentation or by hematogenous tumor spread [33]. High frequency ultrasound may be a very important diagnostic tool in the assessment of these pathologies, their distribution, and relations to the surrounding tissues.

EVUS helps in demonstration of bladder diverticula, foreign bodies in the bladder, and bullous edema. Moreover, this diagnostic procedure allows documentation of functional and morphologic findings, such as position and mobility of the bladder neck.

Urethral mobility, urethral vascularity, funneling of the internal urethral meatus, bladder neck descent, and bladder wall thickness (Fig. 7.15) may be evaluated on pPFUS and EVUS. Not only in patients with stress incontinence, but also in asymptomatic women [42], urethral funneling (UF) may be observed on Valsalva maneuver and sometimes also at rest. Its morphologic basis is unknown and its incidence is reported to range from 18.6% to 97.4%. Funneling is often associated with leakage, and occasionally weak gray-scale echoes may be observed in the proximal urethra, suggesting urine flow and therefore incontinence during straining. However, funneling may also be observed in urge incontinence. Marked funneling has been shown to be associated with poor urethral closure pressures [43, 44]. Tunn et al. [45] performed introital ultrasound in SUI to distinguish patients with and without UF. The two groups were compared for clinical history, urodynamic results, and MRI findings. The results of this study, however, could not elucidate the pathogenesis of UF. The demonstration of UF crucially depends on the examination technique employed [45].

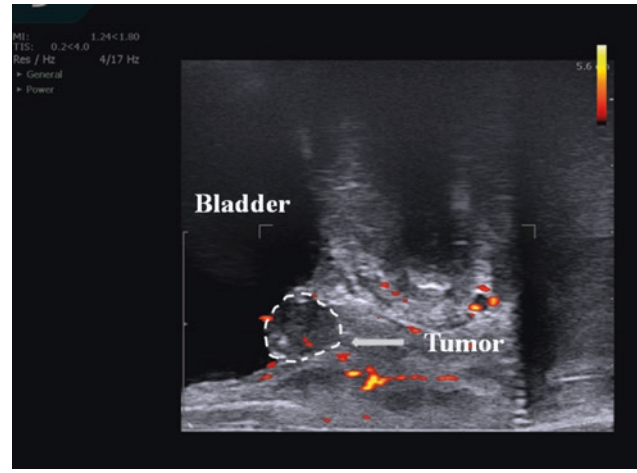

Fig. 7.14 Endovaginal ultrasound with 8848 transducer (BK Ultrasound) demonstrating intraurethral tumor in the area of the proximal urethra

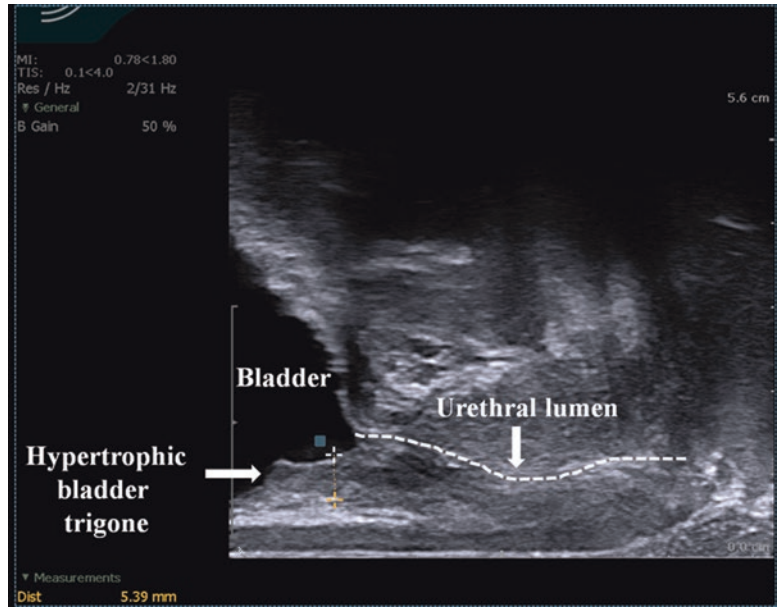

Fig. 7.15 Sagittal section 3D gray-scale image with a biplane 12-MHz transducer (8848, BK Ultrasound). Hypertrophy of the bladder trigone

EVUS is a relatively new technique showing the relations of bladder neck and the urethra. Up-to-date publications concerning these relationships were based mainly on pPFUS, such as the paper published by Schaer et al., who evaluated the bladder neck in continent and stress incontinent women (5 MHz curved linear array transducer) with the help of ultrasound contrast medium (galactose suspension-Echovist-300). This method allowed quantification of the depth and diameter of bladder neck dilation, showing that both incontinent and continent women may have bladder neck dilation and that urinary continence can be established at different locations along the urethra [42]. Parity seemed to be a main prerequisite for a proximal urethral defect with bladder neck dilation. Dietz et al. reported that bladder neck mobility and maximum urethral closure pressure are strong predictors of the diagnosis of urinary stress incontinence, provided that major confounders such as previous incontinence or prolapse surgery, pelvic radiotherapy, or urethral kinking on ultrasound are excluded. Bladder neck descent explains 29% and urethral closure pressure 12% of overall variability. Bladder neck mobility appears to be the strongest predictor [46]. Petros et al. demonstrated that dynamic perineal ultrasound studies show that mid-urethral anchoring of vagina prevents bladder neck descent, funneling, and urine loss on effort. Appearances are consistent with continence control by a musculoelastic mechanism [47].

Hall et al. performed a comparison of periurethral blood flow resistive indices and maximum urethral closure pressure in women with SUI. They reported that translabial ultrasound and Doppler spectral waveform can confidently include assessment of morphology and urethral resistive indices [48].

Khullar et al. [49] described a technique of measuring bladder wall thickness using EVUS. Ultrasonographic measurements showed a good intra- and interobserver reproducibility. Women with urinary symptoms and detrusor instability were found to have significantly thicker bladder walls than women with urodynamically diagnosed stress incontinence. This result was confirmed in another study by the same authors, who reported that a mean bladder wall thickness greater than 5 mm at EVUS is a sensitive screening method for diagnosing detrusor instability in symptomatic women without outflow obstruction [50]. However, in another study performed by Rachaneni et al. it was demonstrated that measuring bladder wall thickness with a transvaginal probe placed at the introitus is not accurate enough to consistently

identify patients with detrusor overactivity and hence cannot be recommended as a replacement test for urodynamic tests [51].

Assessment of the urethral sphincter using a 3D ultrasound scan predicts the outcome of continence surgery [14]. Moreover, in the study by Santiago et al., which aimed to determine the correlation between levator ani deficiency (LAD) and urethral sphincter complex measurements as visualized on 3D endovaginal ultrasonography, and to compare the LAD score with continence status, the authors proved that LAD and urethral sphincter complex status, as visualized on 3D ultrasonography, are independent factors. Moderate to severe LAD is more prevalent in patients with SUI [52]. By performing 3D–pPFUS with the use of a sector endovaginal probe, Digesu et al. found that the RS volume was a predictive factor for surgical outcome [14]. In the study by Klauser et al. performed by dynamic intraurethral sonography with a 12.5-MHz transducer in the diagnostic evaluation of the function of the RS in female patients with urinary stress incontinence in relation to patient age, an age-related decrease in RS function was found [53]. Perucchini et al. suggested that aging is connected to the loss of urethral muscle fibers, which in ultrasonography is observed as increase in echogenicity of the urethra and particularly the RS and/or coexisting decrease in RS volume [54–57]. Post-inflammatory changes may include intra- and periurethral calcifications, fibrosis, and diverticula (Figs. 7.16 and 7.17).

Comparative studies have shown good correlation between pPFUS and radiological methods in the assessment of urinary incontinence and voiding dysfunction [58, 59]. Transperineal/translabial 3D ultrasound is useful to evaluate functional anatomy of the bladder neck and proximal urethra, and to evaluate bladder neck descent (BND), urethral rotation, and the retrovesical angle (RVA) on maximal Valsalva in patients suffering from SUI and urodynamic stress incontinence (USI). It has been proven that BND of 25 mm or higher can be defined as abnormal (hypermobile) on the basis of its association with USI [60]. Translabial ultrasound is also valid in the assessment of the levator–urethra gap, which has the capacity to predict significant prolapse on clinical examination and ultrasound, as well as ballooning of the levator hiatus [61]. Transperineal/translabial ultrasound is discussed in Chap. 3.

There are still no comparative studies between radiological imaging and EVUS, as the latter method is still relatively new. A prospective blind clinical study by Dietz comparing videocystourethrography (VCU) and cystometry, as well as

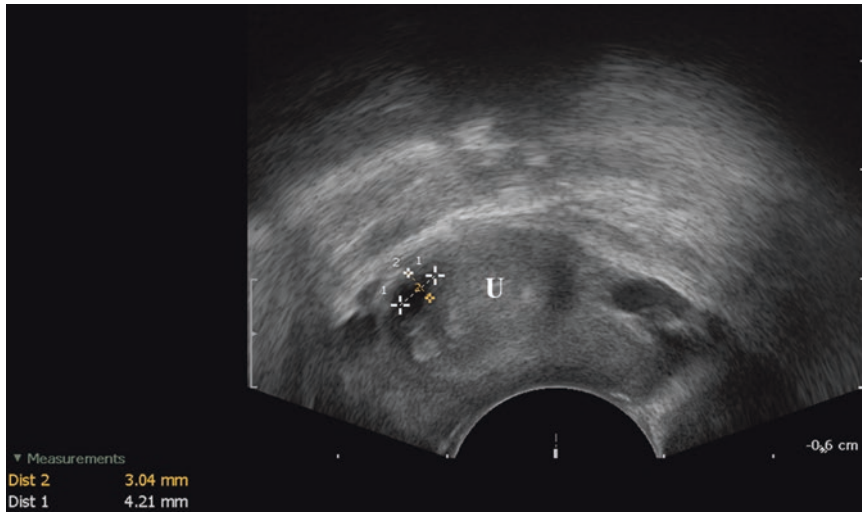

Fig. 7.16 Axial section 2D gray scale with transducer 8848 (BK Ultrasound). Post-inflammatory changes of the urethra—small diverticulum, calcifications, fibrosis, lack of differentiation of the rhabdosphincter

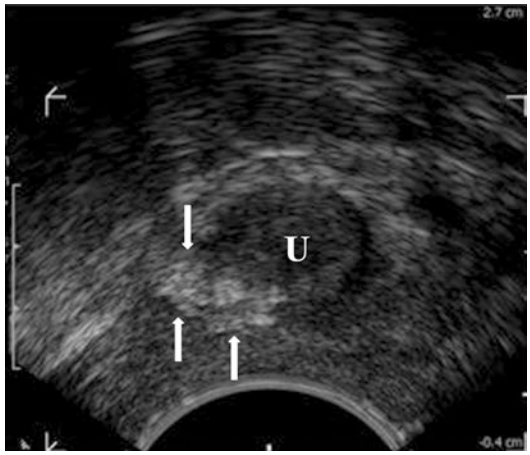

Fig. 7.17 Axial section 3D gray-scale mode, transducer 8848 (BK Ultrasound) image demonstrating urethral calcifications

pPFUS in 125 women, as part of their diagnostic work-up for urinary incontinence or after incontinence-correcting surgery mean bladder neck descent was significantly greater with ultrasound compared to VCU. Rotation of the proximal urethra was not always seen on X-ray, but when it was there was good correlation with ultrasound. There was also good agreement between both tests regarding visualization of funneling or opening of the proximal urethra, with both tests showing equivalent results in 95 out of 117 patients. Overall, a good correlation between ultrasound and radiological findings was observed. Both methods allowed anatomic assessment of the bladder neck and had different strengths and weaknesses. Ultrasound imaging may be preferable; it is cheaper, requires less technological back-up, and avoids the risks of radiation exposure and allergic reactions to contrast medium [58]. Gordon et al. also found good correlation between perineal ultrasound scanning and radiologic scanning of the bladder neck [59]. Lone et. al. have shown that multicompartment ultrasound in the assessment of pelvic floor anatomy is a reliable tool in the anatomical assessment of pelvic floor measurements and POP. The authors found good-to-excellent agreement between the two assessors in the assessment of pelvic floor measurements for all three pelvic floor compartments and suggest that multicompartment pelvic floor ultrasound could be considered as a systematic integrated approach to assess the pelvic floor [62].

Ultrasonography allows evaluation of anti-incontinence procedures and helps in understanding their failure [41]. The study performed by Kociszewski et al. performed with introital ultrasound (3.6–8.3-MHz vaginal probe, 160° ultrasound beam angle) revealed specific ultrasound findings that can be obtained if the tape is either too close to the urethra or too far away and that these findings were associated with a lower cure rate and higher rate of complications. Outcome was best in women in whom ultrasound demonstrated the elastic sling to lie parallel to the urethra at rest and assume a transient C-shape during straining. The authors assumed that this ultrasound finding suggests tension-free orthotopic positioning of the tape and that this position makes optimal use of the tape's elasticity reserve, thereby ensuring sufficient compression of the urethra during Valsalva maneuver. Published data also indicated that if ultrasound showed tape functionality at 6-months, the patient can expect mid-term cure and a low mid-term complication rate [63, 64]. In the study by Bogusiewicz et al. the authors tried to investigate whether the position of the tape under the urethra may influence "outside-in" transobturator sling (TOT) outcome. The study including endovaginal postoperative assessment (Fig. 7.18) with the use of a biplane transducer (type 8848) has shown that the highest failure rate for "outside-in" TOT is associated with the location of the tape under the proximal third of the urethra. Both the middle and distal sections of the urethra may be regarded as targets for transobturator tape placement [65]. In another study by Bascu et al. the authors aimed to evaluate the durability of collagen injection (CI) using serial 3D transvaginal ultrasound in women with sufficient improvement of SUI symptoms not requiring additional treatment. They have demonstrated that, although believed to be nondurable, CI was found to be objectively stable over time by transvaginal 3D ultrasound in a subset of women with durably improved SUI symptoms [66]. A similar study performed by Unger et al. in women with SUI after transurethral injection of Coaptite showed that 90% of patients who underwent Coaptite injection for SUI reported 50% or greater improvement. The volume of Coaptite decreased by 40% over time, and the degree of shrinkage correlated with clinical outcomes [67].

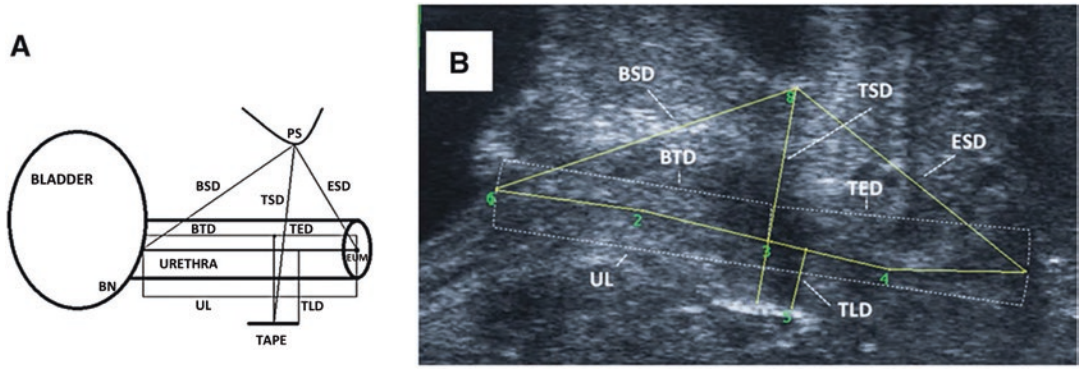

Fig. 7.18 Measurements taken at the sagittal plane: Urethral length (UL), bladder neck–tape distance (BTD), tape–external urethral meatus distance (TED), bladder neck–pubic symphysis distance (BSD), external urethral meatus–pubic symphysis distance (ESD), tape–pubic symphysis distance (TSD), tape–urethral lumen distance (TLD), bladder neck (BN), pubic symphysis (PS), external urethral meatus (EUM). (From Bogusiewicz et al. [65], with permission, published under the Creative Commons Attribution license by SpringerLink and the authors)

Ultrasound is particularly useful in the assessment of postoperative voiding dysfunction. The minimum gap between implant and SP on maximal Valsalva maneuver seems to be the single most useful parameter in the postoperative evaluation of suburethral tapes, as it is associated negatively with voiding dysfunction and positively with both SUI and urge urinary incontinence [68]. Occasionally, sonographic findings will suggest tape perforation (partial or complete) with the implant found within the RS muscle, or even crossing the urethral lumen (Fig. 7.19). At times it is necessary to divide an obstructive tape, and ultrasound can help in locating the tape, as well as in confirming tape division postoperatively [69].

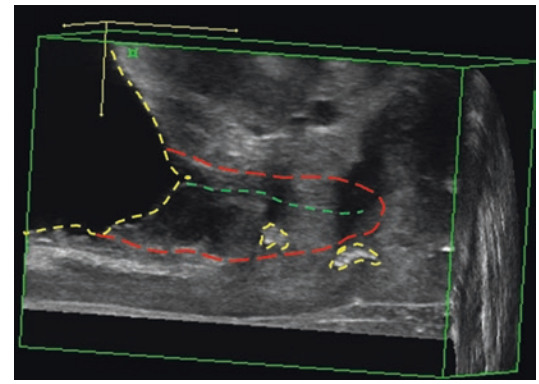

Fig. 7.19 Sagittal section of the urethra with a biplane transducer 8848 (BK Ultrasound) in patient after tape surgery showing two tapes, one inserted into the urethra and another displaced distally

It is important to recognize postoperative changes in the urethra and periurethral tissues and to differentiate these changes from primary urethral disease. Periurethral injection of collagen for SUI can give rise to an echogenic lesion that may be mistaken for a neoplasm. Periurethral calcification can be seen in patients with suture granulomas and in patients who have undergone injection of Durasphere, an injectable agent for SUI. Suture granulomas that develop as a hypersensitivity reaction by the host to suture material may appear as discrete, echogenic foci [70]. Defreitas et al. used endocavitary 3D–ultrasound to examine the distribution of periurethral collagen and to incorporate this technology into a practical treatment decision algorithm for women with SUI requiring collagen injection [71]. Forty-six women who received periurethral collagen injection were assessed with 3D ultrasound 7.5-MHz transvaginal 3D probe placed beneath the urethral meatus to document the position and volume of collagen around the urethra. Patients with a good clinical response were observed with serial 3D ultrasound scans. Circumferential distribution of collagen around the urethra was associated with a higher likelihood of clinical success. The authors found that ultrasonographic evaluation of collagen volume and periurethral location was an affordable, noninvasive, and objective technique to predict improvement after periurethral collagen injection [71].

EVUS is also a very good method for the diagnostics of postoperative complications such as

hematomas (Fig. 7.20) or fistulas (Fig. 7.21). It enables visualization of the pathology, precisely defining its dimensions, distribution, and relation to surrounding structures, and is thus helpful in clinical decisions concerning treatment of the complications. The advantage of the method is also the possibility of detailed assessment in patients who have undergone multiple pelvic floor surgeries (see Fig. 7.20b), as well as complications following vaginal deliveries and obstetrical trauma (Fig. 7.22).

Ultrasonographic imaging findings, however, do not always correlate with clinical findings and patient symptoms, nor does anatomical correction always lead to functional correction. Nevertheless, the goal of pelvic surgery is to

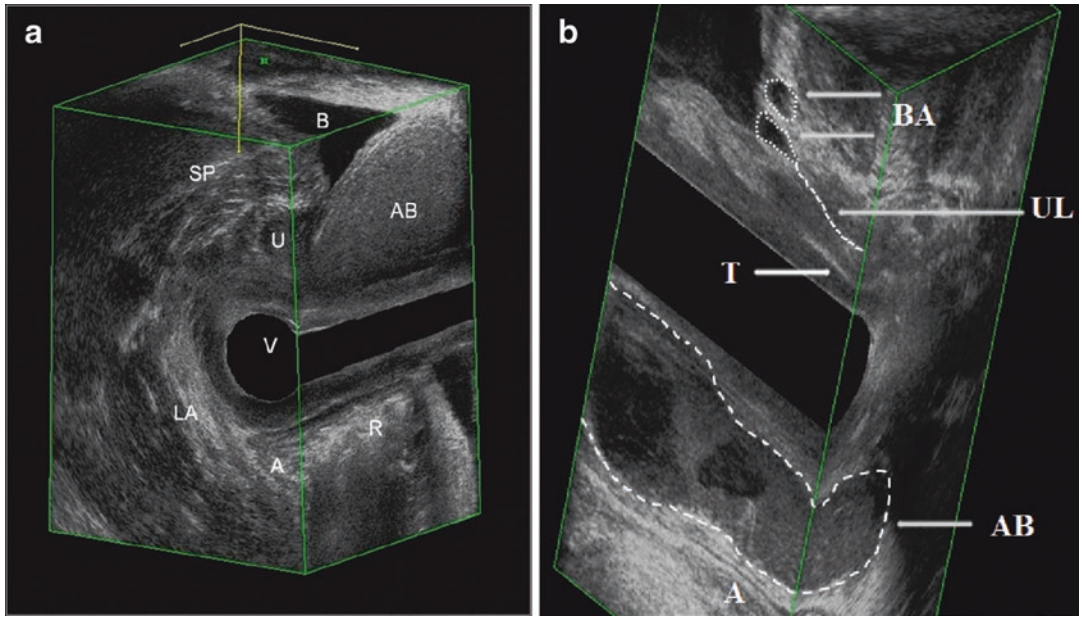

Fig. 7.20 (**a**) Multisurface 3D reconstruction, transducer type 2050 (BK Ultrasound) demonstrating postoperative hematoma. (**b**) Multisurface 3D reconstruction, transducer type 2050 (BK Ultrasound) demonstrating bulking agents protruding to the bladder lumen above the bladder neck, suburethral tape, and retrovaginal abscess. Bulking agents (B), urethral lumen (UL), tape (T), abscess (AB), anal canal (A)

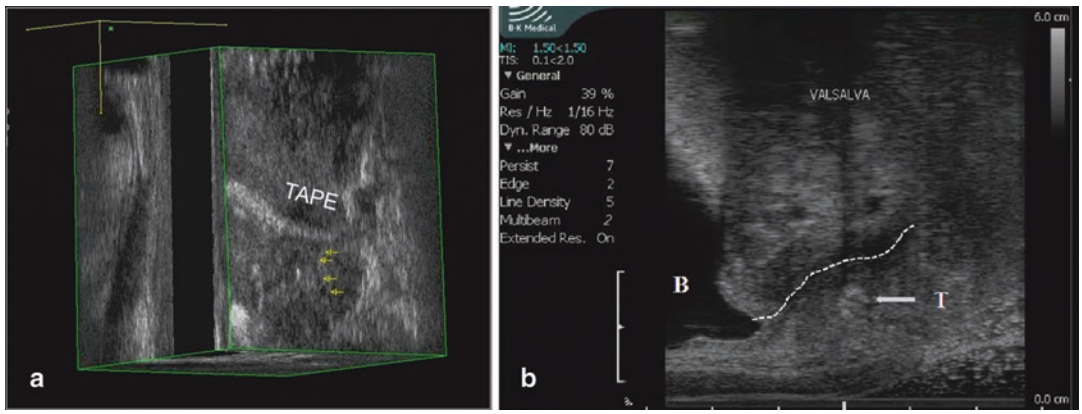

Fig. 7.21 (**a**) Multisurface 3D reconstruction, transducer type 2050 (BK Ultrasound) demonstrating tape, folded and elongated in the distal part, with coexisting postoperative fistula (*arrows*); (**b**) Sagittal section with the transducer type 8848 (BK Ultrasound) during Valsalva maneuver showing the tape protruding to the urethra due to too tight insertion and causing bladder outlet obstruction

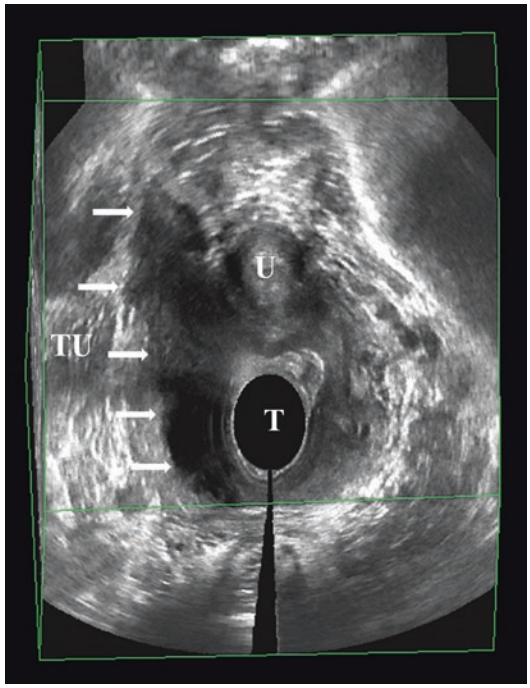

Fig. 7.22 Coronal section 3D gray scale with transducer 8838 (BK Ultrasound). Lack of symmetry, massive thickening of the vaginal wall on the right side due to the obstetrical trauma and episiotomy. Urethra (U), symphysis pubis (SP), vagina (V), transducer (T) in vagina

relieve patient symptoms and to restore anatomy and function whenever possible. There is no doubt that the additional knowledge gained from multicompartmental ultrasonography of the pelvic floor, with a systematic "integrated" approach, will improve our chances of actually reaching this goal. Imaging findings are already leading to either modification of or choice of specific operative procedures [69].

Conclusions and Future Research

3D Endovaginal Ultrasound

3D EVUS using the above-described transducers and high frequency probes enables imaging of the coronal, axial, and oblique sections of the pelvic floor, delivering analytic insight into all pelvic floor structures, including the urethral morphology, defining its normal anatomy or existing abnormalities that may be responsible for pelvic floor disorders. The transducers differ among themselves as to type of data acquisition, different reference points to obtain optimal view, and other details. The electronic character of the crystals and the very high resolution of the obtained images, together with the option for assessing the vascularity of examined organs, have introduced unique imaging opportunities heretofore impossible for all the pelvic floor structures, particularly the urethra and its detailed anatomical and dynamic assessment. The publications by Shobeiri et al. concerning the anatomy of anterior and posterior compartment confirmed with cadaveric studies are a real breakthrough in the attitude to future correlations of the ultrasound morphology, clinical methods, and additional examinations for the understanding of many elements influencing the continence/incontinence in women [12, 18]. It is important to remember that these techniques were described for the first time at the end of the year 2000 [5, 64]. The availability of these transducers is incomparably less than the transducers used for pPFUS, but they have universal character and may be used by many specialties dealing with pelvic floor diseases. The main advantages, apart from the very analytic view of the examined structures, are wider accessibility of ultrasonography than other imaging techniques, simplicity of performance, and ease in understanding and interpreting, together with clinical examination and additional tests.

3D EVUS in Interventional Treatment

The most important application of 3D EVUS of the urethra in understanding and attempting to explain the causes of the high percentage of failures in surgical treatment of patients with urinary incontinence and POP. The influence of the tape and mesh position implemented in the restoration of anatomy continues to be unclear. The opportunity for static and dynamic 3D examinations and their recording will bring new light into the explanation of the causes of surgical failures. The advantage of 3D EVUS is also the assessment of the tension of tapes and their mobility, particularly in patients with postoperation bladder outlet obstruction or voiding dysfunctions. Another

advantage of 3D EVUS is the possibility of detailed assessment of the dimensions and distribution of the postoperative fistulas in the pelvic floor and the possibility of defining the localization and dimensions of abnormal fluid collections such as hematomas or empyemas. It is also crucial to remember that among all available imaging modalities only the ultrasound scanner with biopsy attachment may be used not only in diagnostics and monitoring of treatment but also for interventions in the operating theater. Aspiration of abnormal fluid collections with subsequent lavage and sclerotization can reduce the number of surgical interventions.

Future Applications and Directions of Development

The knowledge of normal and abnormal anatomy of the pelvic floor conditions proper understanding of all these clinically complex processes. Most probably in future years there will be many publications about newly discovered, previously unknown, and not yet described anatomical elements and their relations, not only in the urethra but also in all pelvic floor structures in various groups of clinical disturbances. One of the most important advantages of 2D/3D EVUS of the urethra is the ability to assess vascularization. It is known that pregnancy and labor may deteriorate nerve, muscular, and vascular supply. Recent reports concerning the changes of urethral vascularity, depending on parity, is promising for the future, in comparison to other methods such as urodynamic studies [31]. The possibility of delineating very small ROIs gives hope for creating the opportunity of defining vascularity of tiny organs and their parts, for example RS or other parts of the urethra. 3D EVUS and quantification of vascularity, together with detailed morphological image of urethra, its location, and relations to other organs, may give many new abilities to predict the effectiveness of surgery. Ultrasonography has undergone notable development; 2D techniques develop into 3D; these techniques enable better resolution; they are enriched with dynamic studies, for example, motion tracking and color vector mapping, which enable the assessment of biomechanical properties of tissues and organs. Computer-aided vector-based ultrasound appears to be a feasible and valuable tool for the assessment of bladder neck and urethral mobility and the evaluation of posterior compartment muscle displacement [72, 73]. Another application that might become the modality of the future is elastography of the urethra (Fig. 7.23). This technique, which can map the elastic properties of soft tissue, allowing for differentiation of hard and soft areas, may become useful in diagnostics of urethral pathologies such as tumors, but also might find its role in the diagnostics of urinary incontinence.

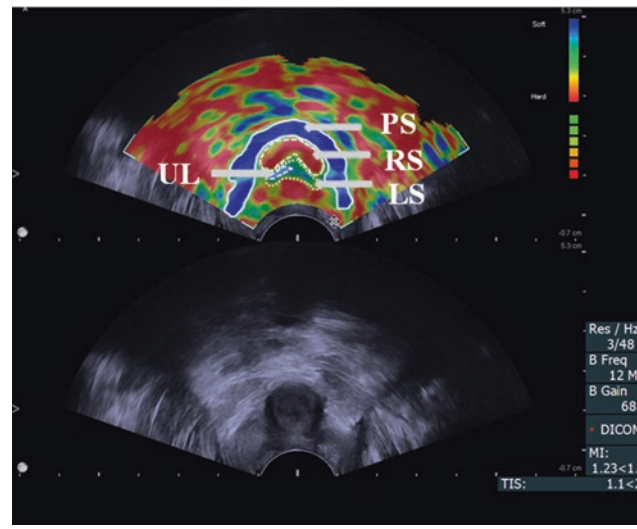

Fig. 7.23 Transvaginal ultrasound with a biplane transducer (Anorectal 3D 20R3, BK Ultrasound) dual mode showing elastographic color map of the urethra (*top*) and the B-mode image of the urethra (*bottom*). Paraurethral structures (PS) *blue* (soft); rhabdosphincter (RS) *red* (hard); lisosphincter (LS) *green* (mid elasticity); urethral lumen (UL) *blue* (soft)

More often the fusion of various image techniques is possible, for example, MR and ultrasound, which may bring new information about morphological and dynamic information about urinary incontinence and POP.

References

1. Petros PE, Ulmsten UI. An integral theory and its method for the diagnosis and management of female urinary incontinence. Scand J Urol Nephrol Suppl. 1993;153:1–93.
2. Petros PE, Ulmsten UI. An integral theory of female urinary incontinence. Experimental and clinical considerations. Acta Obstet Gynecol Scand Suppl. 1990;153:7–31.
3. Petros PE, Woodman PJ. The integral theory of continence. Int Urogynecol J Pelvic Floor Dysfunct. 2008;19(1):35–40.
4. Santoro GA, Wieczorek AP, Shobeiri SA, Mueller ER, Pilat J, Stankiewicz A, et al. Interobserver and interdisciplinary reproducibility of 3D endovaginal ultrasound assessment of pelvic floor anatomy. Int Urogynecol J. 2011;22(1):53–9.
5. Santoro GA, Wieczorek AP, Stankiewicz A, Woźniak MM, Bogusiewicz M, Rechberger T. High-resolution three-dimensional endovaginal ultrasonography in the assessment of pelvic floor anatomy: a preliminary study. Int Urogynecol J Pelvic Floor Dysfunct. 2009;20(10):1213–22.
6. Haylen BT, de Ridder D, Freeman RM, Swift SE, Berghmans B, Lee J, et al. An International Urogynecological Association (IUGA)/International Continence Society (ICS) joint report on the terminology for female pelvic floor dysfunction. Neurourol Urodyn. 2010;29(1):4–20.
7. Toozs-Hobson P, Freeman R, Barber M, Maher C, Haylen B, Athanasiou S, et al. An International Urogynecological Association (IUGA)/International Continence Society (ICS) joint report on the terminology for reporting outcomes of surgical procedures for pelvic organ prolapse. Neurourol Urodyn. 2012;31(4):415–21.
8. Stankiewicz A, Wieczorek AP, Woźniak MM, Bogusiewicz M, Futyma K, Santoro GA, Rechberger T. Comparison of accuracy of functional measurements of the urethra in transperineal vs. endovaginal ultrasound in incontinent women. Pelviperineology. 2008;27:145–7.
9. Santoro GA, Fortling B. The advantages of volume rendering in three-dimensional endosonography of the anorectum. Dis Colon Rectum. 2007;50(3):359–68.
10. Santoro GA, Wieczorek AP, Shobeiri SA, Stankiewicz A. Endovaginal ultrasonography: methodology and normal pelvic floor anatomy. In: Santoro GA, Wieczorek AP, Bartram CI, editors. Pelvic floor disorders: imaging and multidisciplinary approach to management. Dordrecht: Springer; 2010. p. 61–78.
11. Wieczorek AP, Woźniak MM, Stankiewicz A, Santoro GA, Bogusiewicz M, Rechberger T. 3-D high-frequency endovaginal ultrasound of female urethral complex and assessment of inter-observer reliability. Eur J Radiol. 2012;81(1):e7–12.
12. Shobeiri SA, Leclaire E, Nihira MA, Quiroz LH, O'Donoghue D. Appearance of the levator ani muscle subdivisions in endovaginal three-dimensional ultrasonography. Obstet Gynecol. 2009;114(1):66–72.
13. Petros PP. Medium-term follow-up of the intravaginal slingplasty operation indicates minimal deterioration of urinary continence with time. Aust N Z J Obstet Gynaecol. 1999;39(3):354–6.
14. Digesu GA, Robinson D, Cardozo L, Khullar V. Three-dimensional ultrasound of the urethral sphincter predicts continence surgery outcome. Neurourol Urodyn. 2009;28(1):90–4.
15. Umek WH, La T, Stutterecker D, Obermair A, Leodolter S, Hanzal E. The urethra during pelvic floor contraction: observations on three-dimensional ultrasound. Obstet Gynecol. 2002;100(4):796–800.
16. Umek WH, Obermair A, Stutterecker D, Hausler G, Leodolter S, Hanzal E. Three-dimensional ultrasound of the female urethra: comparing transvaginal and transrectal scanning. Ultrasound Obstet Gynecol. 2001;17(5):425–30.
17. Derpapas A, Ahmed S, Vijaya G, Digesu GA, Regan L, Fernando R, et al. Racial differences in female urethral morphology and levator hiatal dimensions: an ultrasound study. Neurourol Urodyn. 2012;31(4):502–7.
18. Shobeiri SA, White D, Quiroz LH, Nihira MA. Anterior and posterior compartment 3D endovaginal ultrasound anatomy based on direct histologic comparison. Int Urogynecol J. 2012;23(8):1047–53.
19. Kondo Y, Homma Y, Takahashi S, Kitamura T, Kawabe K. Transvaginal ultrasound of urethral sphincter at the mid urethra in continent and incontinent women. J Urol. 2001;165(1):149–52.
20. Macura KJ, Genadry R, Borman TL, Mostwin JL, Lardo AC, Bluemke DA. Evaluation of the female urethra with intraurethral magnetic resonance imaging. J Magn Reson Imaging. 2004;20(1):153–9.
21. Frauscher F, Helweg G, Strasser H, Enna B, Klauser A, Knapp R, et al. Intraurethral ultrasound: diagnostic evaluation of the striated urethral sphincter in incontinent females. Eur Radiol. 1998;8(1):50–3.
22. Haderer JM, Pannu HK, Genadry R, Hutchins GM. Controversies in female urethral anatomy and their significance for understanding urinary continence: observations and literature review. Int Urogynecol J Pelvic Floor Dysfunct. 2002;13(4):236–52.
23. Howard D, Delancey JO, Tunn R, Ashton-Miller JA. Racial differences in the structure and function of the stress urinary continence mechanism. Obstet Gynecol. 2000;95(5):713–7.
24. Ashton-Miller JA, DeLancey JO. Functional anatomy of the female pelvic floor. Ann N Y Acad Sci. 2007;1101:266–96.
25. Caine M. Peripheral factors in urinary continence. J Urol (Paris). 1986;92(8):521–30.

26. Jackson SR, Brookes S, Abrams P. Measuring urethral blood flow using Doppler ultrasonography. BJU Int. 2000;86(7):910–7.
27. Siracusano S, Bertolotto M, d'Aloia G, Silvestre G, Stener S. Colour Doppler ultrasonography of female urethral vascularization in normal young volunteers: a preliminary report. BJU Int. 2001;88(4):378–81.
28. Siracusano S, Bertolotto M, Cucchi A, Lampropoulou N, Tiberio A, Gasparini C, et al. Application of ultrasound contrast agents for the characterization of female urethral vascularization in healthy pre- and postmenopausal volunteers: preliminary report. Eur Urol. 2006;50(6):1316–22.
29. Wieczorek AP, Woźniak MM, Stankiewicz A, Santoro GA, Bogusiewicz M, Rechberger T, et al. Quantitative assessment of urethral vascularity in nulliparous females using high-frequency endovaginal ultrasonography. World J Urol. 2011;29(5):625–32.
30. Wieczorek AP, Woźniak MM, Stankiewicz A, Bogusiewicz M, Santoro GA, Rechberger T, Scholbach J. The assessment of normal female urethral vascularity with color Doppler endovaginal ultrasonography: preliminary report. Pelviperineology. 2009;28:59–61.
31. Lone F, Sultan AH, Stankiewicz A, Thakar R, Wieczorek AP. Vascularity of the urethra in continent women using colour doppler high-frequency endovaginal ultrasonography. SpringerPlus. 2014;3:619. doi:10.1186/2193-1801-3-619.
32. Lone F, Thakar R, Wieczorek AP, Sultan AH, Stankiewicz A. Assessment of urethral vascularity using 2D colour Doppler high-frequency endovaginal ultrasonography in women treated for symptomatic stress urinary incontinence: 1-year prospective follow-up study. Int Urogynecol J. 2016;27(1):85–92.
33. Chaudhari VV, Patel MK, Douek M, Raman SS. MR imaging and US of female urethral and periurethral disease. Radiographics. 2010;30(7):1857–74.
34. Albers P, Foster RS, Bihrle R, Adams MC, Keating MA. Ectopic ureters and ureteroceles in adults. Urology. 1995;45(5):870–4.
35. Wang S, Lang JH, Zhou HM. Symptomatic urinary problems in female genital tract anomalies. Int Urogynecol J Pelvic Floor Dysfunct. 2009;20(4):401–6.
36. Tunn R, Schaer G, Peschers U, Bader W, Gauruder A, Hanzal E, et al. Updated recommendations on ultrasonography in urogynecology. Int Urogynecol J Pelvic Floor Dysfunct. 2005;16(3):236–41.
37. Yang JM, Huang WC, Yang SH. Transvaginal sonography in the diagnosis, management and follow-up of complex paraurethral abnormalities. Ultrasound Obstet Gynecol. 2005;25(3):302–6.
38. Kawashima A, Sandler CM, Wasserman NF, LeRoy AJ, King Jr BF, Goldman SM. Imaging of urethral disease: a pictorial review. Radiographics. 2004;24(Suppl 1):S195–216.
39. Huang WC, Yang SH, Yang SY, Yang E, Yang JM. Vaginal abscess mimicking a cystocele and causing voiding dysfunction after burch colposuspension. J Ultrasound Med. 2009;28(1):63–6.
40. Rostaminia G, White DE, Quiroz LH, Shobeiri SA. Visualization of periurethral structures by 3D endovaginal ultrasonography in midsagittal plane is not associated with stress urinary incontinence status. Int Urogynecol J. 2013;24(7):1145–50.
41. Yang JM, Yang SH, Huang WC. Two- and three-dimensional sonographic findings in a case of distal urethral obstruction due to a paraurethral tumor. Ultrasound Obstet Gynecol. 2005;25(5):519–21.
42. Schaer GN, Perucchini D, Munz E, Peschers U, Koechli OR, Delancey JO. Sonographic evaluation of the bladder neck in continent and stress-incontinent women. Obstet Gynecol. 1999;93(3):412–6.
43. Dietz HP. Ultrasound imaging of the pelvic floor. Part I: two-dimensional aspects. Ultrasound Obstet Gynecol. 2004;23(1):80–92.
44. Huang WC, Yang JM. Bladder neck funneling on ultrasound cystourethrography in primary stress urinary incontinence: a sign associated with urethral hypermobility and intrinsic sphincter deficiency. Urology. 2003;61(5):936–41.
45. Tunn R, Goldammer K, Gauruder-Burmester A, Wildt B, Beyersdorff D. Pathogenesis of urethral funneling in women with stress urinary incontinence assessed by introital ultrasound. Ultrasound Obstet Gynecol. 2005;26(3):287–92.
46. Dietz HP, Clarke B, Herbison P. Bladder neck mobility and urethral closure pressure as predictors of genuine stress incontinence. Int Urogynecol J Pelvic Floor Dysfunct. 2002;13(5):289–93.
47. Petros PP, Von Konsky B. Anchoring the midurethra restores bladder-neck anatomy and continence. Lancet. 1999;354(9183):997–8.
48. Hall RJ, Rogers RG, Saiz L, Qualls C. Translabial ultrasound assessment of the anal sphincter complex: normal measurements of the internal and external anal sphincters at the proximal, mid-, and distal levels. Int Urogynecol J Pelvic Floor Dysfunct. 2007;18(8):881–8.
49. Khullar V, Salvatore S, Cardozo L, Bourne TH, Abbott D, Kelleher C. A novel technique for measuring bladder wall thickness in women using transvaginal ultrasound. Ultrasound Obstet Gynecol. 1994;4(3):220–3.
50. Khullar V, Cardozo LD, Salvatore S, Hill S. Ultrasound: a noninvasive screening test for detrusor instability. Br J Obstet Gynaecol. 1996;103(9):904–8.
51. Rachaneni S, McCooty S, Middleton LJ, Parker VL, Daniels JP, Coomarasamy A, Bladder Ultrasound Study (BUS) Collaborative Group, et al. Bladder ultrasonography for diagnosing detrusor overactivity: test accuracy study and economic evaluation. Health Technol Assess. 2016;20(7):1–150.
52. Santiago AC, O'Leary DE, Quiroz LH, Shobeiri SA. Is there a correlation between levator ani and urethral sphincter complex status on 3D ultrasonography? Int Urogynecol J. 2015;26(5):699–705.
53. Klauser A, Frauscher F, Strasser H, Helweg G, Kolle D, Strohmeyer D, et al. Age-related rhabdosphincter function in female urinary stress incontinence: assessment of intraurethral sonography. J Ultrasound Med. 2004;23(5):631–7.. quiz 8–9

54. Perucchini D, DeLancey JO, Ashton-Miller JA, Galecki A, Schaer GN. Age effects on urethral striated muscle. II. Anatomic location of muscle loss. Am J Obstet Gynecol. 2002;186(3):356–60.
55. Perucchini D, DeLancey JO, Ashton-Miller JA, Peschers U, Kataria T. Age effects on urethral striated muscle. I. Changes in number and diameter of striated muscle fibers in the ventral urethra. Am J Obstet Gynecol. 2002;186(3):351–5.
56. Wieczorek AP, Woźniak MM, Stankiewicz A. Ultrasonography. In: Santoro GA, Wieczorek AP, Bartram CI, editors. Pelvic floor disorders: imaging and multidisciplinary approach to management. Dordrecht: Springer; 2010. p. 175–87.
57. Santoro GA, Wieczorek AP, Woźniak MM, Stankiewicz A. Endoluminal ultrasonography. In: Santoro GA, Wieczorek AP, Bartram CI, editors. Pelvic floor disorders: imaging and multidisciplinary approach to management. Dordrecht: Springer; 2010. p. 389–403.
58. Dietz HP, Wilson PD. Anatomical assessment of the bladder outlet and proximal urethra using ultrasound and videocystourethrography. Int Urogynecol J Pelvic Floor Dysfunct. 1998;9(6):365–9.
59. Gordon D, Pearce M, Norton P, Stanton SL. Comparison of ultrasound and lateral chain urethrocystography in the determination of bladder neck descent. Am J Obstet Gynecol. 1989;160(1):182–5.
60. Naranjo-Ortiz C, Shek KL, Martin AJ, Dietz HP. What is normal bladder neck anatomy? Int Urogynecol J. 2016;27(6):945–50.
61. Dietz HP, Garnham AP, Rojas RG. Is the levator-urethra gap helpful for diagnosing avulsion? Int Urogynecol J. 2016;27(6):909–13.
62. Lone F, Sultan AH, Stankiewicz A, Thakar R. Interobserver agreement of multicompartment ultrasound in the assessment of pelvic floor anatomy. Br J Radiol. 2016;89(1059):20150704. doi:10.1259/bjr.20150704.
63. Kociszewski J, Rautenberg O, Kolben S, Eberhard J, Hilgers R, Viereck V. Tape functionality: position, change in shape, and outcome after TVT procedure–mid-term results. Int Urogynecol J. 2010;21(7):795–800.
64. Kociszewski J, Rautenberg O, Perucchini D, Eberhard J, Geissbuhler V, Hilgers R, et al. Tape functionality: sonographic tape characteristics and outcome after TVT incontinence surgery. Neurourol Urodyn. 2008;27(6):485–90.
65. Bogusiewicz M, Monist M, Gałczyński K, Woźniak M, Wieczorek AP, Rechberger T. Both the middle and distal sections of the urethra may be regarded as optimal targets for 'outside-in' transobturator tape placement. World J Urol. 2014;32(6):1605–11.
66. Bacsu CD, Cunningham C, Christie A, Zimmern PE. Durability of collagen injection for stress urinary incontinence in women proven by transvaginal 3-dimensional ultrasound. Female Pelvic Med Reconstr Surg. 2015;21(1):25–9.
67. Unger CA, Barber MD, Walters MD. Ultrasound evaluation of the urethra and bladder neck before and after transurethral bulking. Female Pelvic Med Reconstr Surg. 2016;22(2):118–22.
68. Chantarasorn V, Shek KL, Dietz HP. Sonographic appearance of transobturator slings: implications for function and dysfunction. Int Urogynecol J. 2011;22(4):493–8.
69. Santoro GA, Wieczorek AP, Dietz HP, Mellgren A, Sultan AH, Shobeiri SA, et al. State of the art: an integrated approach to pelvic floor ultrasonography. Ultrasound Obstet Gynecol. 2011;37(4):381–96.
70. Prasad SR, Menias CO, Narra VR, Middleton WD, Mukundan G, Samadi N, et al. Cross-sectional imaging of the female urethra: technique and results. Radiographics. 2005;25(3):749–61.
71. Defreitas GA, Wilson TS, Zimmern PE, Forte TB. Three-dimensional ultrasonography: an objective outcome tool to assess collagen distribution in women with stress urinary incontinence. Urology. 2003;62(2):232–6.
72. Santoro GA, Shobeiri SA, Scholbach J, Chlebiej M, Wieczorek AP. Technical innovations in pelvic floor ultrasonography. In: Santoro GA, Wieczorek AP, Bartram CI, editors. Pelvic floor disorders: imaging and multidisciplinary approach to management. Dordrecht: Springer; 2010. p. 103–14.
73. Reddy AP, DeLancey JO, Zwica LM, Ashton-Miller JA. On-screen vector-based ultrasound assessment of vesical neck movement. Am J Obstet Gynecol. 2001;185(1):65–70.